April 2015

Metapopulation Dynamics of the Northern Spotted Owl

David Michael Eufemia
Worcester Polytechnic Institute

Project Number: MQP-SDO-205

Patchy Dynamics

A Major Qualifying Project Report

Submitted to The Faculty

of

Worcester Polytechnic Institute

In partial fulfillment of the requirements for the

Degree of Bachelor of Science

by

David Eufemia

April, 2015

Approved:

Professor Sarah Olson

Abstract

Metapopulations are becoming more prevalent across all species. The complex relationships between these species and their environments can be mapped using the basic metapopulation equation created by Levins. In order to capture a more realistic description for the northern spotted owl specifically, this equation was further developed into a system of three ordinary differential equations. This system of equations more accurately described the variations in the northern spotted owls patch occupancy. This was accomplished by introducing parameters which were shown to have largely unexplored relationships with the rates of extinction and colonization. After finding some strong correlations between parameters and their effects on the owls patch occupancy, it is clear that the northern spotted owl needs more data to be collected in order to develop an accurate and working model.

Executive Summary

The dynamics of patchy habitats are becoming increasingly valuable to study as more species tend towards developing metapopulations. The most basic models for describing the dynamics between these patches are the Levins model and the mainland-island model. Both these models utilize far too many assumptions however, and their ability to be applied to real world problems remains minimal. Fortunately, these models are excellent foundations to developing more sophisticated equations which can be specialized for use with a species or group of populations of interest. One such example is this project's development of a system of three ordinary differential equations in order to describe the patch dynamics of the endangered northern spotted owl. The northern spotted owl is a species of special interest because their threatened state is largely due to the timber industry removing old-growth forests across North America. As a species whose fate was largely influenced by acts of humanity, success in the form of preservation of the species would be a tremendous triumph.

The system of differential equations utilized to describe the behavior of these beings incorporates data specific to the northern spotted owl which was chosen because it produced the largest effects on this species ability to function as metapopulations. The data which was able to be readily applied to the northern spotted owl included fecundity, rainfall, as well as a parameter for the varying patch sizes. The rainfall data was incorporated after LaHaye's observation that 52% of the variation in fecundity could be attributed to rainfall. Preliminary attempts at describing rainfall included attempting to fit sine curves in order to capture the variation in rainfall from year to year. Unfortunately, attempting to describe the data in this fashion yielded uninspiring results which did not capture the droughts or periods of excess rainfall. The rainfall data instead needed to be altered into a rainfall metric to be used for the system of differential equations. First the data needed to be taken for the period beginning in June and ending in May. This constituted a year and matched up more accurately with the northern spotted owl's mating period. The rainfall data was then transformed into the rainfall metric by comparing the current year's rainfall with that of the previous five years as well as the average for the entire target period. This allowed for a determination of whether or not the owl's required more or less rainfall than average which then led to either a positive rainfall metric if they matched up (for example if the owl needed extra rainfall and that year had more rainfall than average) or a negative rainfall metric if they did not. Finally the rainfall data was then scaled down to the interval [-1,1] in order to facilitate ease with introducing it to the system of equations.

Fecundity was incorporated in order to help describe variations in colonization rate, a rate which in previous models was held to be constant. Fecundity and the rate of change of fecundity are the two key parameters that have the greatest impact on the rate of change of the colonization rate. Both these terms needed to be accounted for in order to fully capture the effect on local colonization since there should be a larger effect when both fecundity and rate of change of fecundity are large than when fecundity is small and rate of change of fecundity is large. The equations for rate of change of fecundity and rate of change of colonization are both sigmoidal functions meaning that they act as saturation functions in order to prevent extreme values. Ultimately this model and future models need access to much more field data about the northern spotted owl in order to accurately capture the species' dynamics in a patchy environment.

Acknowledgements

I would like to take this opportunity to offer my sincere thanks to my advisor Professor Sarah Olson for her unceasing encouragement and support as well as her invaluable guidance and expertise throughout this project. Her exceptional passion not only for mathematics but for helping others in times of need is inspirational and something I hope to emulate as I pursue my future career.

Contents

List of Figures

Chapter 1

Introduction and Motivation

1.1 Metapopulations Overview

Metapopulations are rapidly becoming more prevalent as humanity continues to modify landscapes in the struggle to support ever-increasing populations. As such, studying the dynamics between these populations is increasing in importance for those who wish to preserve the Earth's biodiversity. Although metapopulations can occur naturally as some species have adapted very specialized habitats, those resulting from anthropogenic impacts are of chief concern. Traditionally the individuals comprising these species would have movements and interactions which are continuous. However, due to overexploitation of the environment by humans, habitats have increasingly deteriorated into "spatially disjunct patches separated by intervening unsuitable habitat"[26]. As the main cause of the dire circumstances these species now find themselves, with extinction rates thousands of times higher than the estimated background rates, it is the responsibility of humanity to join them in their fight for survival [7].

1.2 Metapopulation Models

1.2.1 Levins and Mainland-Island Models

The term metapopulation first arose in 1969 by Richard Levins while he studied pest control policies; however, before this there were several papers which explored how a single local population site could frequently go extinct and recolonize while the population as a whole survived [20]. Levins was able to distinguish his work by developing a model to describe the rate of change of p (fraction of occupied habitat patches at time t) in terms of two independent parameters m and e (rates for local colonization and extinction respectively both with units of $\frac{1}{time}$). His original model was

$$\frac{dp}{dt} = mp(1-p) - ep, \tag{1.1}$$

where the first term ($mp(1-p)$) represents the increasing portion of the equation which is determined by combining the colonization rate with the fraction of patches already occupied and the fraction of patches that can still be colonized. This highlights the relationship behind how colonizing more patches lends itself to colonizing less patches as there will be less patches available to colonize. The second term (ep) on the other hand is simply the rate at which patches already colonized become locally extinct. This term only depends on the fraction of patches colonized since the uncolonized patches will not affect local extinction and thus $\frac{dp}{dt}$.

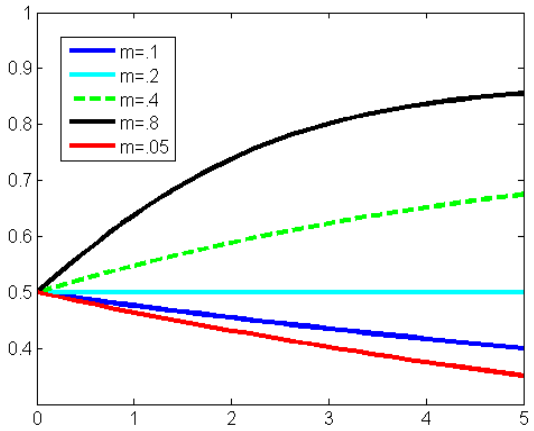

Figure 1.1: Levins model from Eq.(1.1) with constant extinction rate of $e = 0.1$ while varying colonization rates and with initial condition for occupied habitat patches as $p = 0.5$.

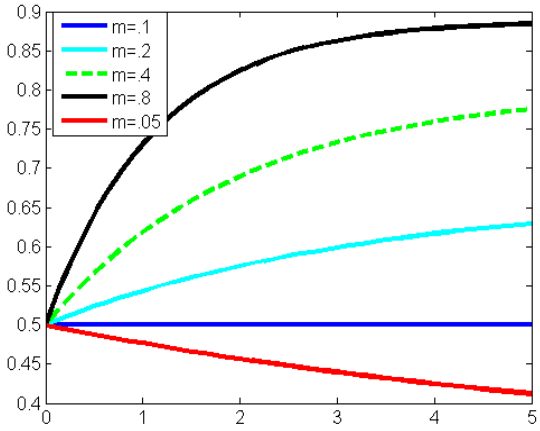

Figure 1.2: Mainland-island model from Eq.(1.3) with constant extinction rate of $e = 0.1$ while varying colonization rates and with initial condition for occupied habitat patches as $p = 0.5$.

This model incorporates the idea that in order for the persistence of the population as a whole, m must be greater than e which produces an equilibrium value, $\bar{p} > 0$ at

$$\bar{p} = \frac{(m-e)}{m} = 1 - \frac{e}{m} \tag{1.2}$$

where due to the limitations of m and e, $\bar{p}$ must be greater than or equal to zero for $m \leq e$. In Fig. 1.1 we see an equilibrium develops at $\bar{p} = \frac{7}{8}$, $\bar{p} = \frac{3}{4}$, and $\bar{p} = \frac{1}{2}$ for $m = 0.8$, $m = 0.4$, and $m = 0.2$ respectively while the other two values of m cause the model to tend towards zero. Fig. 1.1 shows that the equilibrium point does not increase uniformly with colonization and instead begins to display behavior that tends to be less sensitive as the colonization rate reaches extreme values.

Levins model is an alteration of the mainland-island population model since metapopulations can be conceptualized as island habitats in a sea of unsuitable habitat. Unfortunately the mainland-island model does not describe the edges of habitats well as they are generally gradient on land as opposed to the drastic and sudden change from an island to the surrounding water. The mainland-island model [20] is

$$\frac{dp}{dt} = m(1-p) - ep, \tag{1.3}$$

with an equilibrium point at

$$\bar{p} = \frac{m}{m+e}. \tag{1.4}$$

From Eq. (1.4) we can see equilibriums develop at $\bar{p} = \frac{8}{9}$, $\bar{p} = \frac{4}{5}$, $\bar{p} = \frac{2}{3}$, $\bar{p} = \frac{1}{2}$, and $\bar{p} = \frac{1}{3}$ for $m = 0.8$, $m = 0.4$, $m = 0.2$, $m = 0.1$, and $m = 0.05$ respectively. The model's behavior of tending towards these equilibriums for these values of colonization rate m are illustrated in Fig. 1.2. One notable difference from Levins model is that these new equilibrium values never reach zero. In fact the only way for the mainland-island model to reach an equilibrium of zero is for the colonization rate to be equal to zero.

In order to further emphasize the similarities between the Levins model and the mainland-island model, each was graphed in Fig. 1.3 with varying colonization rates while the initial fraction of patches occupied and extinction rate were held constant at $p = 0.5$ and $e = 0.1$. It is clear from Fig. 1.3 that

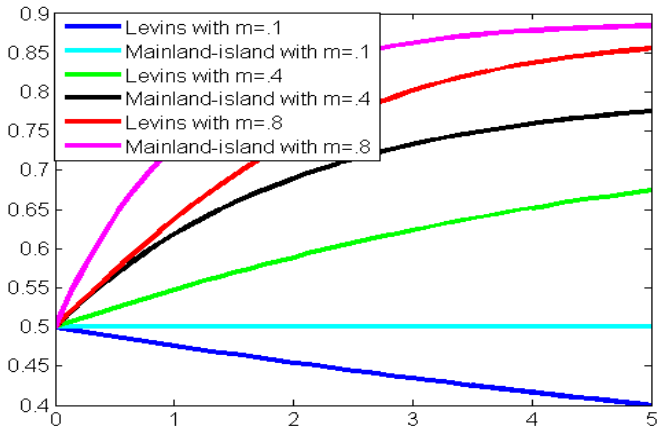

Figure 1.3: Levins and mainland-island model comparison with constant extinction rate of $e = 0.1$ while varying colonization rates and with initial condition for occupied habitat patches as $p = 0.5$.

each of the Levins curves have lower equilibriums than the mainland-island curve with the corresponding colonization rate. The Levins model generally appears to have an equilibrium 0.1 less than the mainland-island model, however as the models approach equilibriums nearing one (or zero which is not shown in Fig. 1.3) the equilibriums begin to close in on each other.

In order to simplify comparison to another significant model, Hanski and Gilpin rewrote Levins original model in order to show that it is structurally the same as a logistic growth model [20]. This re-written equation was expressed as

$$\frac{dp}{dt} = (m - e)p\left[1 - \frac{p}{1 - \frac{e}{m}}\right]. \tag{1.5}$$

Unfortunately the Levins model has several simplifying assumptions built into it which drastically damages its ability to be applied to real world populations [27, 36]. These include:

1. The population density of habitats is assumed to either be zero or carrying capacity (From Hanski's rewritten version carrying capacity can be observed to be $1 - \frac{e}{m}$).
2. The spatial arrangement of the patches is ignored (particularly evident in how every local population maintains the same extinction and recolonization rates).
3. There are a large number of patches.
4. Carrying capacity between local populations is constant.
5. The habitat patches are all similar in both size and quality.
6. All habitat patches are suitable for occupancy.
7. Dispersal success is limited to a single transition or single search for a new habitat.

1.2.2 Modified Levins Models

Several models have attempted to improve the Levins model for real world applications by relaxing some of these assumptions. One such attempt was by Noon et al. (1996) who designed a model which relaxed assumptions 6 and 7 in order to alter the likelihood of successful dispersal (in the Levins model successful dispersal is proportional to $1 - p$) [27]. First, a parameter h was added which represented the proportion of habitat patches suitable for occupancy relaxing assumption 6. Relaxing assumption 7 yielded a parameter n which represented the number of patches to be searched during dispersal. The new equation was written as

$$\frac{dp}{dt} = mp\left[1 - [(1-h) + ph]^n\right] - ep, \tag{1.6}$$

and represented a new level of complexity in order to better describe the real world.

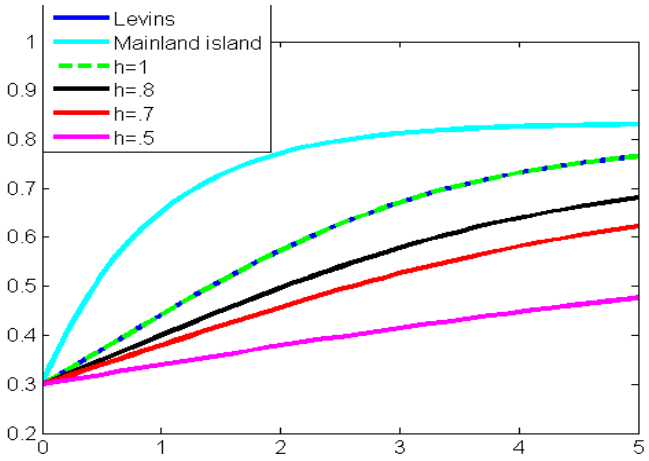

Figure 1.4: Comparison of Levins from Eq.(1.1), mainland-island from Eq.(1.3), and Eq.(1.6) with varying h parameter and initial condition for occupied habitat patches as $p = 0.3$.

In this equation (Eq. (1.6)), when $n = h = 1$, it becomes the original Levins model since $n = 1$ represents only allowing a single transition and $h = 1$ represents all habitat patches being suitable for occupancy. This behavior is observed in Fig 1.4. The Mainland island model, on the other hand, displays a tendency to yield higher equilibrium values than Levins and its extension Eq. (1.6) for similar colonization and extinction rates. The lower values of h show that as there are less patches suitable for occupancy, the equilibrium level decreased as well, which is the expected behavior. This variation of the Levins model allows for the increased search ability to compensate for the portion of patches now deemed unacceptable for occupancy; thus reducing the risk of all local populations experiencing extinction due to some sort of catastrophic event. Fig. 1.5 shows successful dispersal when n patches are allowed to be searched compared to when only a single transition for searches is allowed. The tendency of this term shows that simply allowing four patches to be searched rather than a single transition period nearly guarantees successful dispersal under this model. In Fig. 1.6 we can observe how increasing the value of n leads to an increased equilibrium level (where increasing n from 1 to 2 yields a higher equilibrium value for Eq. (1.6) than for both the Levins and the mainland-island models).

Although the Levins model incorporates several assumptions which hurt its ability to describe real-life applications, it also requires the least amount of data (when compared to models which incorporate geo-referenced data) [11]. This makes it especially convenient to use for analyzing the viability of

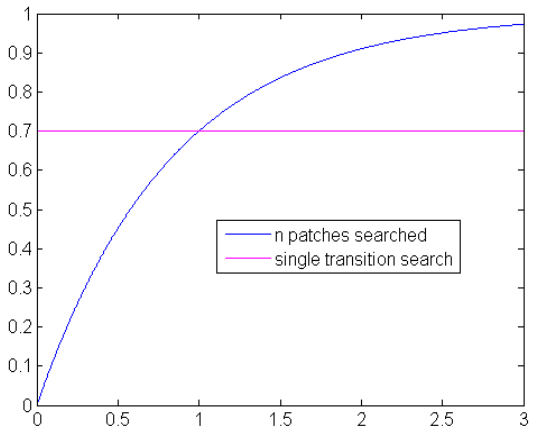

Figure 1.5: Comparison of dispersal success terms from Eq.(1.1) and Eq.(1.6).

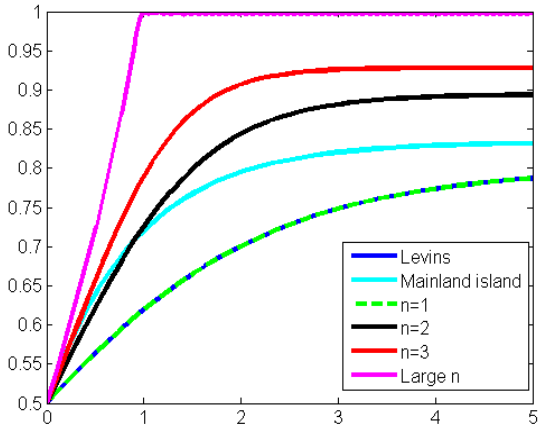

Figure 1.6: Comparison of Levins from Eq.(1.1), mainland-island from Eq.(1.3), and Eq.(1.6) with varying n parameter and initial condition for occupied habitat patches as $p = 0.5$.

populations. Specifically, these models can help conservationists determine relative collapse points for populations. These are points where the local populations have a probability of extinction but a trivial probability of recolonization; leading to the inevitable extinction of the entire population. By obtaining a general knowledge of where these thresholds may lie, conservationists are able to take preventative measures in order to sustain the populations of these species for the long term. The data required for applying the Levins model can be difficult to measure however, as it can prove to be challenging determining values for the extinction and colonization rates as well as identifying the local populations [33]. Harrison (1991) even attempted to further classify metapopulations as belonging to one of four groups. These include:

1. Non-equilibrium Metapopulations: A collection of small patches with high extinction probabilities compared to recolonization.

2. Classical Model: A collection of small patches that may be prone to local extinction however due to their location relative to other patches they have a recolonization rate which balances with the extinction.

3. Patchy Metapopulations: A collection of patches with high migration due to close proximity allowing them to act as a continuous distribution in the long-run.

4. Mainland-Island Model: A collection of both large and small patches close enough to allow frequent migration from an extinction-resistant mainland.

Although many species in nature do not easily fit into a single designation, these groups allow a general description of some of the patterns that occur most frequently. However in order to combat this problem, Smith et al. (1996) determined that the local populations could instead be better described as either an island, midland, or mainland. The designation of island would apply to highly extinction-prone subpopulations; mainland would describe subpopulations which are large enough to be invulnerable to extinction; while midland would be used for intermediate subpopulations. One method which is

employed in order to identify subpopulations is to look at the genetics of the species (since the local populations will necessarily have more genetic similarities due to the fact that, by definition, their within-patch dynamics should be higher than their between-patch dynamics).

1.2.3 Lande Model

In addition to the Levins model, another popular model for metapopulations was developed by Lande. This model (also known as the territory model) tracks birth and death rates at the scale of the individual where Levins, on the other hand, tracks the colonization and extinction rates of local populations. The Lande model incorporates the Euler-Lotka equation (Eq.(1.7)) and a term for successfully dispersing juveniles (Eq.(1.8))

$$R_0 = b\sum_{x=0}^{\infty} l_x b_x = 1, \tag{1.7}$$

$$J_D = 1 - [(1-h) + ph]^n, \tag{1.8}$$

where p once again represents the fraction of patches occupied, h describes the fraction of patches that are suitable for occupation, n represents the number of patches each juvenile is able to search, R_0 represents the lifetime reproduction of female offspring per female, b denotes average fecundity (the number of female offspring produced per female) for the entire population, b_x represents fecundity at age x, and l_x represents the probability of survival to age x [27]. Lande applied a two-stage model (with juveniles and adults) to the Euler-Lotka equation which yields a solution of

$$R_0 = s_0 \frac{b}{1-s}, \tag{1.9}$$

with s_0 denoting the survival probability to age 1 and s the average survival probability of adults. Finally the combination of Eq.(1.9) and Eq.(1.8) yields Lande's model to find an equilibrium, denoted as $\bar{p}$ in the equation

$$[1 - [(1-h) + \bar{p}h]^n]R_0' = J_D \cdot R_0' = 1. \tag{1.10}$$

Eq.(1.10) incorporates an alternative form of R_0 which removes survival probability to age one to describe the juvenile population and instead utilizes the term J_D for successful dispersal. This attribute better defines the population which will survive as adults since unsuccessful dispersal is generally a death sentence. This new symbol is denoted R_0' and is simply

$$R_0' = \frac{b}{1-s}. \tag{1.11}$$

This combination is best described explicitly in that the equilibrium is calculated by taking Eq.(1.9), or the life history of the species, and then removing the probability of survival to age one and instead using the term for successful juvenile dispersal which more accurately describes the juveniles who will flourish in a suitable territory.

Unfortunately this model is unable to capture stochastic fluctuations in the rates of fecundity and survival probability; similar to the problems the Levins model encounters with variations in extinction and colonization. However, Lande's model utilizes parameters that are easily quantifiable in survival probability and fecundity as opposed to extinction and colonization. Since Lande's model works at the individual level it also prevents discrepancies which arise when defining areas as local patches. Levins also assumes that local patch dynamics occur on a much faster time scale than between-patch while Lande's model has no difference in time scales.

1.2.4 Hanski Models

In order to describe the colonization term in Levins model, Hanski used a parameter for successful colonization coupled with a parameter for immigration [18]. These modified terms were incorporated into a system of three differential equations. This model, like Levins, assumes that all local populations are equal in size, however, the equilibrium population size is affected by dispersal in addition to local dynamics. A key to this model is that the time scale of local dynamics are assumed to be much faster than those of between-patches. The model is

$$\frac{dp}{dt} = \alpha\beta I(1-p) - ep, \tag{1.12}$$

$$\frac{dN}{dt} = -mN + \alpha I + rN(1-N), \tag{1.13}$$

$$\frac{dI}{dt} = mpN - vI - \alpha I, \tag{1.14}$$

where I is the number of dispersers per habitat patch, α is the immigration parameter, β is the probability of successful dispersal, v is the rate of mortality of dispersers, N is local population size, and r is population growth rate.

Diamond (1975) found that the probability of species inhabiting an island was dependent on island area. In order to capture this relationship, Hanski (1993) developed a modified Levins model which also incorporated a parameter a to describe the range of patch sizes,

$$\frac{dp}{dt} = m\left[(1+a)\frac{p}{a+p}\right](1-p) - e\left[\frac{a}{1+a} + \frac{p}{a+p}\right]p, \tag{1.15}$$

where an increasing value of a denotes a decrease in the frequency of large patches and, consequently, a decrease in the colonization term. This model, rather than contrasting the Levins and Mainland models, instead combined them as extremes on a continuum (the mainland-island model representing the maximum for steady-state equilibrium and the Levins model representing the minimum). As seen in Fig. 1.7, in this model when $a = 0$ it becomes the mainland-island model and when $a \to \infty$ it becomes the Levins model.

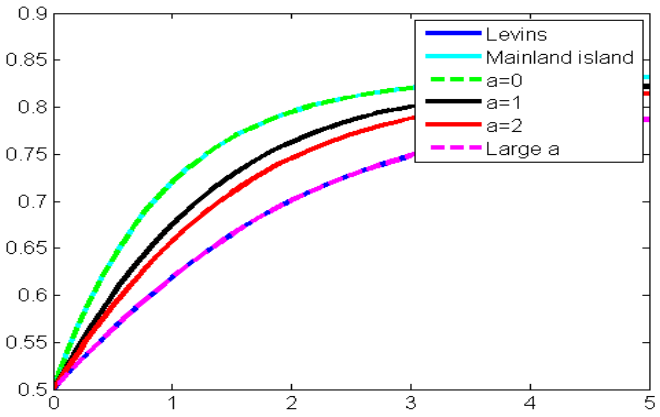

Figure 1.7: Comparison of Levins from Eq.(1.1), mainland-island from Eq.(1.3), and Eq.(1.15) with varying a parameter and initial condition for occupied habitat patches as $p = 0.5$.

This model encounters a rescue effect [21]. The rescue effect describes the phenomena that occurs in this model where as p increases, the extinction term decreases. Hanski (1993) suggested that this phenomena is likely due to the fact that this model assumes the time scales for local and between-patch dynamics to be similar.

Computer-based spatial models are another form of model which, due to their influence over decision makers, deserve to be mentioned. These models permit behavior to be described explicitly. However, they require extensive high quality data since slight errors can produce drastic variation [11].

Chapter 2

Data

2.1 Spotted Owl

This project will address several of the problems associated with the Levins model and attempt to design a better model geared specifically towards protecting the spotted owl (Strix occidentalis caurina observed in Fig. 2.1). The framework for this new model will begin with Eq.(1.15) while designing a system of differential equations to describe the variations of the colonization rate. This results in a new model with parameters describing the patches based on factors originating from the individuals. In this way, the time scale of the patches is made to be similar to the time scale of the individual.

Figure 2.1: Strix occidentalis caurina in native environment [5].

The spotted owl is a species which thrives only in old forest growth areas of at least 80 years [4]. This habitat, unfortunately, is also ideal for logging since these areas are dense with timber. Due to over-exploitation from logging, these areas have become drastically reduced in size and fragmented leading the spotted owl to develop metapopulations. When forced to overpopulate a small or ill-fitting habitat, the owls become at risk to suffer from starvation, predation, and the populations become susceptible to natural disasters. Spotted owls became classified as a threatened species by the U.S. government in 1990, which affords them some protection from logging (40% of habitat within a 1.3 mile radius of a nest cannot be destroyed) [3]. Unfortunately, the spotted owl population has continued to decline approximately 4% per year [35]. Recently the barred owl has also begun to threaten the spotted owl as

a competitor which is better suited to adapting to the declines in habitat quality [30]. The spotted owls generally have developed source-sink dynamics between patches as a result of their territorial nature. Spotted owls from high quality patches produce emigrants who migrate to low quality patches where populations cannot sustain themselves without more immigration. Fig. 2.2 depicts an example of a range of known patches in southern California.

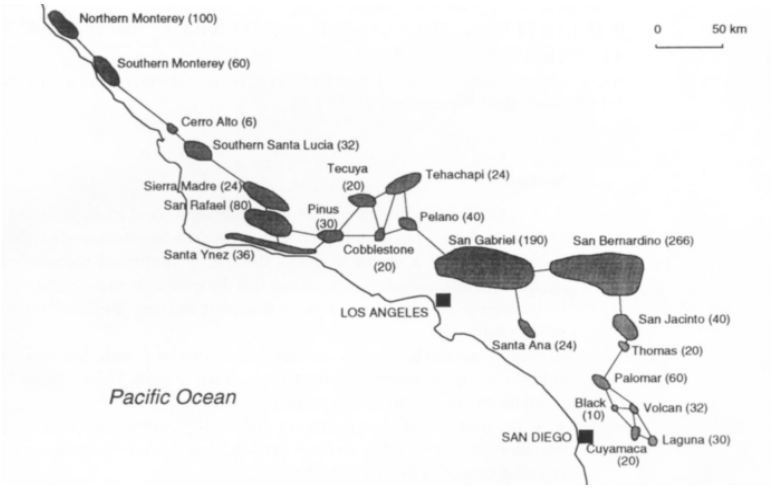

Figure 2.2: Spotted owl southern Californian habitat patches [24].

2.2 Rainfall and Fecundity Relationship

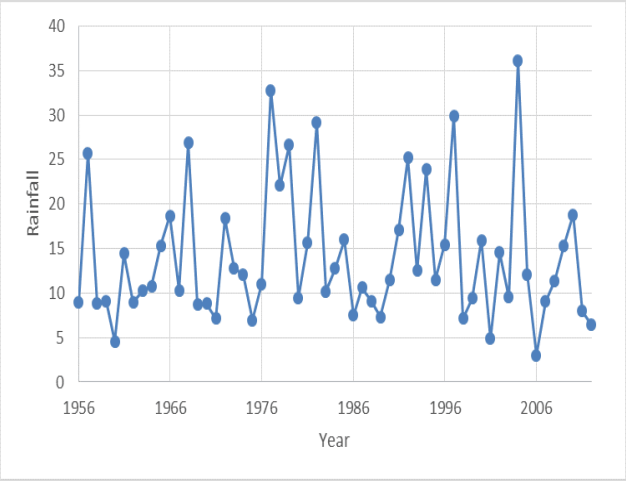

Figure 2.3: The rainfall data (from [1]) used to simulate the changes in fecundity.

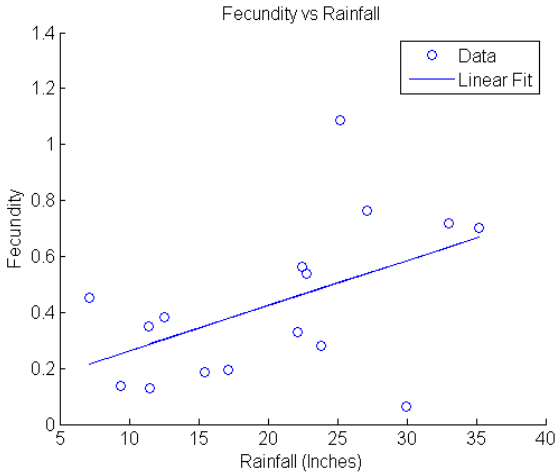

Figure 2.4: Comparison of the relationship between fecundity and rainfall with linear fit.

Data was collected in order to develop a specialized model for the spotted owl. Colonization rate, limited by the available data, was set to depend on fecundity. One relationship of note which was found by Lahaye et al. (1994) was that approximately 52% of variation in fecundity could be attributed to variations in yearly rainfall (the year beginning in June and ending in May). Data accumulated by Lahaye et al. (1994) and Blakesley et al. (2001) are combined with rainfall data (Fig. 2.3) in Fig. 2.4.

This led to developing a function to describe rainfall in relation to time. One attempt was to fit a sine function

$$SF = 14.4413 + 4.0630 \cdot \sin(1.4791 \cdot t + 5.0600) \tag{2.1}$$

to the data from the past twenty years since the general trend appeared to be oscillations. Unfortunately this attempt, which is shown in Fig. 2.5, did not yield particularly accurate results (the R^2 value for this best fit sine curve was only 0.13). Although this function had a higher R^2 value, a variation (Fig. 2.6) with

$$SF = -0.2912 \cdot t + 17.4257 + 13.2414 \cdot \sin(1.0798 \cdot t + 5.7185) \tag{2.2}$$

managed to better capture the overall range of points and the oscillations. This function also acts in accordance to the prediction by Peery et al. (2012) that climate change will have a general effect of decreasing the amount of precipitation in regions occupied by the spotted owl. This trend of decreasing average precipitation levels was added to the function in the form of a negative linear term in Eq.(2.2). The parameters for Eq.(2.1) and Eq.(2.2) were developed in Matlab using the Fit technique. First the Fittype function was utilized to develop the unique functions from Eq.(2.1) and Eq.(2.2). Then the Fit function utilizes the least squares method in which the distance between the actual data points and the predicted value by the function (at the same time value) is squared (in order to make all distances the same sign) and then each squared distance is summed. The goal of this method is to get the lowest summation, meaning that the distance between the predicted values and the actual values is small. For this application, the Fit function utilizes the least squares method for many varying values of the parameters and provides the values for the parameters which returned the smallest summed squared distances. An example of the code incorporated for Eq.(2.2) is shown below.

```
Sine = fittype('a*x+p+b*sin(c*x+d)',...
    'dependent',{'y'},'independent',{'x'},...
    'coefficients',{'a','p','b','c','d'});
% coefficients
Fit = fit(x,y,Sine,'StartPoint',[-.2,18,10,2*pi/6,pi/2]);
```

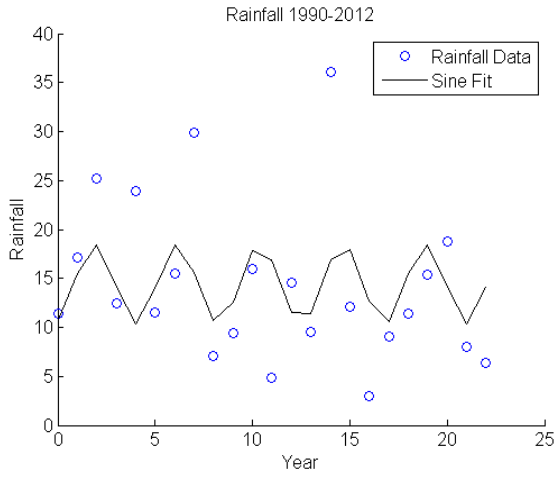

Figure 2.5: Rainfall from 1990-2012 with fitted sine curve from Eq.(2.1).

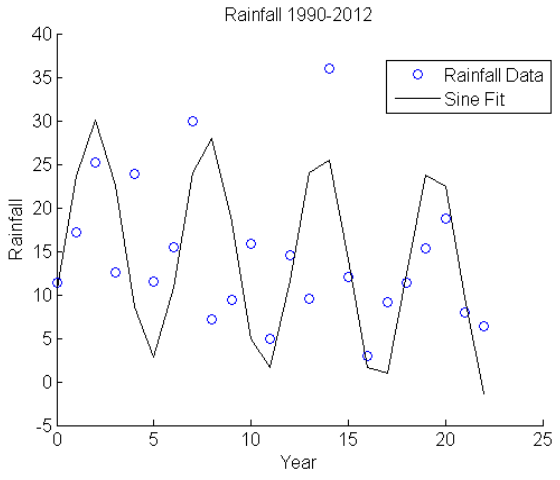

Figure 2.6: Rainfall from 1990-2012 with fitted negatively linear sine curve from Eq.(2.2).

Although LaHaye et al. (1994) found the variation in fecundity to be largely dependent on rainfall, his conclusion was based on an extremely small sample size. When including data from Blakesley et al.

(2001), (Fig. 2.4 with equation $F = 0.0161 \cdot \mathcal{R} + 0.1015$ where F denotes fecundity and $\mathcal{R}$ represents rainfall) the R^2 value (which is calculated by $R^2 = 1 - \frac{SSE}{SST}$ where SSE represents the sum of the squared errors and SST represents the sum of the squared values for the actual data, as this value approaches 1.00 the data is being more accurately described by the model) decreases to only 0.2440. However a closer examination of the data reveals three points which may be considered special cases. Fig. 2.7 ($F = 0.0225 \cdot \mathcal{R} - 0.0512$) is the result of removing these points resulting in an R^2 value of 0.6781. The first of these special cases occurred in 1992 when the fecundity exploded to over 1.08. This may have been due to the fact that for the ten years prior the total rainfall was consistently lower values, never exceeding 20 inches (Average rainfall for this period was only 11.34 inches). However in 1992 the rainfall was 25.22 inches effectively ending the "drought period" before leading to the fecundity of the spotted owls exploding. The second case occurred in 1997-1998 when the opposite sequence occurred. This time the past 5 years had heavy rainfall (average of 19.74 inches) culminating in a 29.92 inch year in 1997 where the fecundity dropped to only 0.065. However in 1998 when the rainfall again fell, the fecundity instead jumped, this time to 0.454. This shows that, based on the available data, fecundity is dependent on not only that year's rainfall, but also the rainfall of prior years. Fecundity appears to drop when rainfall becomes either excessive or scarce based on the previous years. Following these periods, during a year which contradicts the previous trend of either too much or too little rainfall, the fecundity then appears to jump to higher levels. In order to capture this trend it appeared to be necessary to develop a rainfall metric which not only describes the current year, but also those from the previous years.

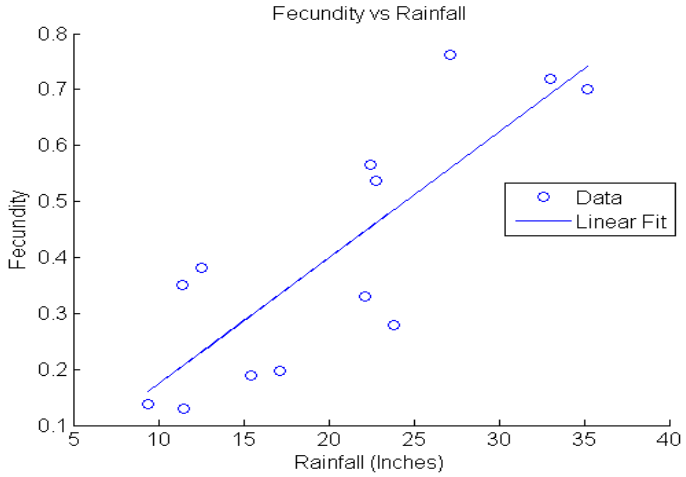

Figure 2.7: Comparison of the relationship between fecundity and rainfall with two data points excluded and linear fit.

Since preliminary attempts at using a Sine function to describe rainfall led to the extended periods of drought and flood being removed, a rainfall metric was developed. This rainfall metric was determined to be based on average rainfall over the previous five years in relation to the average rainfall for the total period of twenty-eight years as well as rainfall for the target year. The average rainfall for the five years previous to a target year would be compared to the average for the entire twenty-eight year period (in order to capture the difference between target years which required excess rainfall and those which required levels lower than average). If the average for the previous five years was greater than the average for the entire period, then the rainfall metric would be positive (meaning in theory it would positively affect the fecundity rates) for the target year only if the rainfall for that year was less than

the average for the entire period. Conversely, if the rainfall for the target year and the five-year average were both in excess of the average for the entire period, then the rainfall metric would yield a negative value (signifying that the fecundity rates would be negatively affected). Similarly, if the average for the previous five years was less than the average for the entire period then the reverse would occur (target years with rainfall greater than the average for the entire period would then yield the positive rainfall metrics). This was accomplished through the use of

$$RRM = (\overline{FY} - \overline{EP}) \cdot (\overline{EP} - TY), \tag{2.3}$$

where RRM denotes the raw rainfall metric before scaling, $\overline{FY}$ represents the average rainfall for the previous five years, $\overline{EP}$ signifies the average rainfall for the entire period, and TY denotes the rainfall for the target year. The raw rainfall metric was then scaled to a range of [-1,1] in order to ease its introduction into the equations. This scaling was accomplished by using the equation

$$f(x) = \frac{(b-a)(x-min)}{max-min} + a \tag{2.4}$$

where x is the current years rainfall, min is the minimum amount of rainfall during the period of interest, max represents the maximum amount of rainfall during the target period, a is the minimum of the scaled range (in this case -1), and b describes the maximum of the scaled range (in this case 1).

Similarly to the observation by LaHaye et al. (1994) that 52% of variation in fecundity could be attributed to rainfall, Peery et al. (2012) found that approximately 85% of variation in survival rates was due to rainfall. This lends survival rates to be described using a similar rainfall function as the one used for fecundity. However, as seen in Fig. 2.8, the rates for survival appear to remain relatively constant between years and may be better described by using varying values within a range of [0.75,1] (this is reinforced by the estimated survivorships seen in Fig. 2.9, Fig. 2.10, and Fig. 2.11). There does appear to be a difference in survival between juveniles and adults as seen in Fig. 2.10 and Fig. 2.11, which may need to be considered.

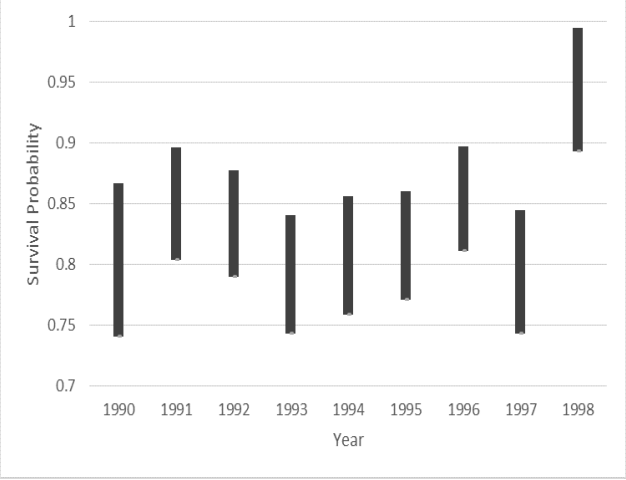

Figure 2.8: The estimated apparent survival of non-juvenile spotted owls in northeastern California from [6].

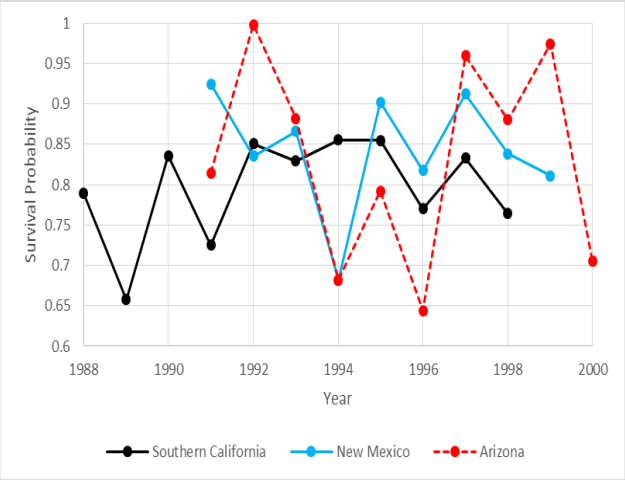

Figure 2.9: Estimated survival probability from 1987 to 2001 taken from [29].

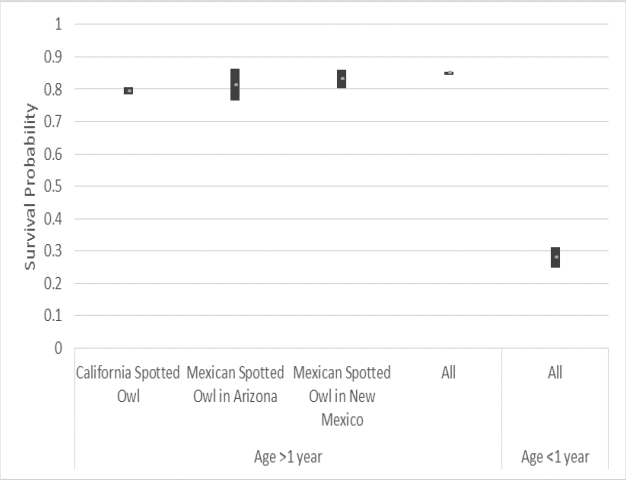

Figure 2.10: The apparent survival probability of spotted owls in California, Arizona, and New Mexico taken from [6].

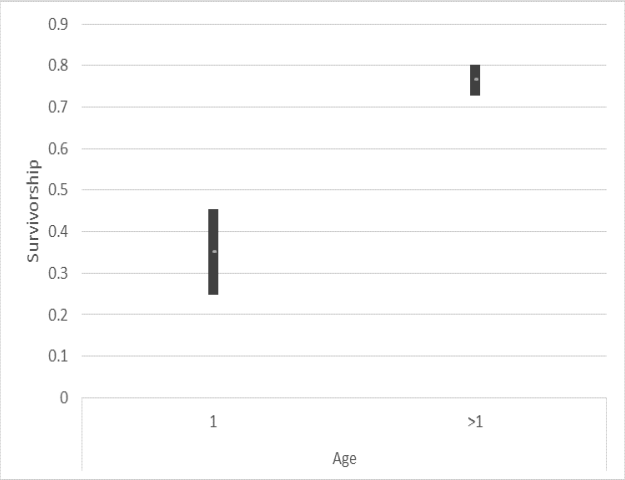

Figure 2.11: The estimated survivorship of spotted owls with 95% confidence interval used by [24].

Chapter 3

System of Ordinary Differential Equations

3.1 Fraction of Patches

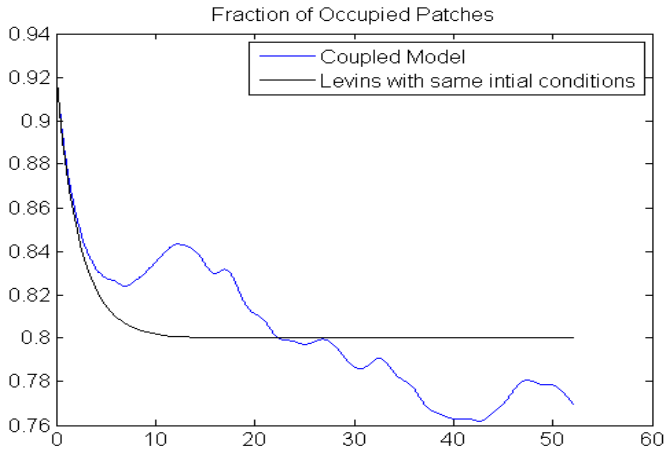

Figure 3.1: Fraction of patches occupied with respect to time for the new model ($a = 0$ and $e = 0.1$) and Levins model.

In order to design an accurate model specific to the northern spotted owl, the species' environmental relationships needed to be accounted for. The new model has a foundation in the original Levins model, Eq. (1.1). This singular equation was then coupled with two other equations to form a system of ordinary differential equations. The first equation,

$$\frac{dp}{dt} = M(u, g, F, p)\left[(1+a)\frac{p}{a+p}\right](1-p) - e\left[\frac{a}{1+a} + \frac{p}{a+p}\right]p, \tag{3.1}$$

is the same as Eq.(1.15) as it allowed for the description of the range of patch sizes to become incorporated. In this equation p has no units as it is a fraction, likewise a has no units, and M and e both have units of $\frac{1}{\text{time}}$ in order for $\frac{dp}{dt}$ to have units of $\frac{1}{\text{time}}$. As evidenced in Fig. 3.1, this new model incorporates the kinds of variation that the Levins model cannot. This is key because the initial conditions supplied to the model should not determine the equilibrium that the population will tend towards fifty years later since these values are subject to change. The initial condition for the fraction of patches occupied

was taken from estimates of owl occupation in habitats derived from field data from California, Wisconsin, and Oregon by Thomas (1990). These habitats have descriptions included in the study however there is no mention of carrying capacity which is an assumption that is fundamental to Levins model, and consequentially, this model.

3.2 Fecundity

The second equation describes the changes in fecundity (the number of female offspring produced per female). In order to capture changes in fecundity, the model needed to incorporate the environmental factors which may influence its value both directly and indirectly. Unfortunately due to lack of available field data, this left the relationship found by Perry et al. (2012) which explored how rainfall influenced fecundity. These relationships are expressed by

$$\frac{dF}{dt} = q(RM, t), \tag{3.2}$$

which shows the change in fecundity is based on time and the developed rainfall metric. Preliminary attempts to develop an expression to describe $\frac{dF}{dt}$ led to

$$\frac{dF}{dt} = k \cdot RM, \tag{3.3}$$

where k is simply a parameter and RM denotes the rainfall metric. This model was deemed unacceptable however, because it yielded fecundity values which either increased too greatly or decreased too greatly resulting in values outside an acceptable range for the fecundity (either below zero or consistently greater than about 0.5). In order to attempt to narrow the values to a more acceptable range, the equation

$$\frac{dF}{dt} = \frac{k \cdot RM}{RM + L} \tag{3.4}$$

was developed. This equation still describes the rate of change in fecundity based largely on the rainfall metric, denoted RM. However, unlike the last attempt, this equation also contains two parameters k and L whose values are crucial in yielding usable data. Eq.(3.4) utilizes fecundity as F which by definition has units of $\frac{\text{number of female offspring}}{\text{number of females}}$ and RM has no units; thus L similarly has no units and k has units of $\frac{\text{number of female offspring}}{\text{number of females·time}}$ in order for $\frac{dF}{dt}$ to have units of $\frac{\text{number of female offspring}}{\text{number of females·time}}$. Appropriate values appear to be approximately $k = 0.2$ and $L = 2$ for the data used in this instance (as shown in Fig. 3.2). However it is important to note that these values are specific to the data they describe since there are many different factors not accounted for in the model (due to lack of sufficient data in addition to the owls responding differently to other environmental influences). For the data used in this project, values that deviate too greatly from the absolute value of those previously mentioned yield unrealistic values for fecundity, in which the fecundity of the owls is predicted to drop below zero. Fig. 3.2 also shows that not all the variation in fecundity was able to be captured, specifically the value from the actual data of over one, however the general range of the majority of the actual data was accurately described and the value greater than one may be viewed as an outlier. Another serious problem that needs to be monitored in Eq.(3.4) is the possibility for the denominator to be valued as zero. This can be avoided by preventing L from having an absolute value less than or equal to one since the rainfall metric was scaled to occupy the interval [-1,1]. The structure of this equation is based on creating sigmoidal behavior in the rate of change of fecundity. This prevented the previous problem

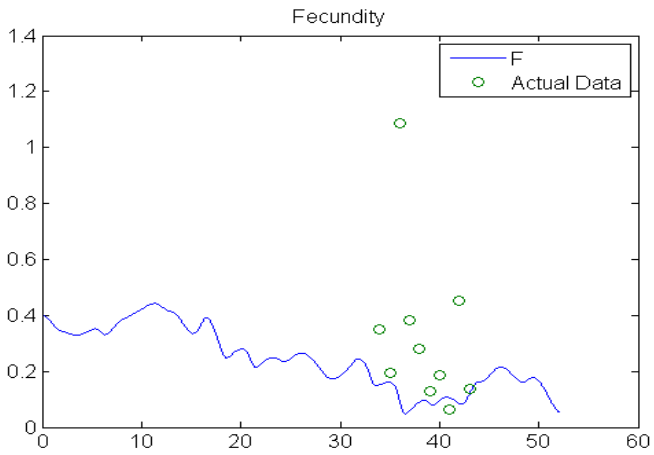

Figure 3.2: Fecundity with respect to time ($k = 0.2$ and $L = 2$).

of the values escaping acceptable ranges. The basic equation of this type is called the Hill equation which is of the form

$$y = \frac{y_m \cdot x^\alpha}{c^\alpha + x^\alpha} \tag{3.5}$$

where in our usage $y_m = k$, $\alpha = 1$, $y = \frac{dF}{dt}$, $x = RM$, and $c = L$ [14].

3.3 Colonization Rate

The final equation in this system was developed in order to vary the colonization rate. In order to capture variations in this rate the model needed to again consider the influence of environmental factors. This led to exploring the relationship found by LaHaye et al. (1994) which demonstrated that rainfall effects the survival rate of the northern spotted owl. However after further investigation, the variations in survival were small enough that they were deemed to be acceptably removed from consideration (although greater survival rates from the previous year would suggest that the colonization rate should increase since there would be more owl's surviving in patches and needing to relocate). The foundation of the colonization equation is

$$\frac{dM}{dt} = h\left(\frac{dF}{dt}, F, t, p\right) \tag{3.6}$$

which demonstrates that the change in colonization rate is based on the change in fecundity, fecundity itself, time, and the fraction of patches occupied. However, preliminary attempts did not consider these factors. The first attempt at an equation was

$$\frac{dM}{dt} = \frac{RM}{RM + g} \cdot u \tag{3.7}$$

where RM denotes the rainfall metric while u and g both represent parameters with certain units. Unfortunately by defining the change in colonization rate in this way it displayed behavior that was almost identical to the behavior of fecundity developed by Eq.(3.4). This was deemed unacceptable after further exploration because colonization was more appropriately described by the change in fecundity rather than the variable which the change in fecundity was determined to be chiefly based upon (the

colonization rate's connection to change in fecundity can be viewed by looking at a large change in fecundity as meaning that the amount of juveniles who will be dispersing will be greater). Using the change in fecundity as a substitute for the rainfall metric yielded

$$\frac{dM}{dt} = \frac{\frac{dF}{dt}}{\frac{dF}{dt} + g} \cdot u \tag{3.8}$$

which with manipulation of the parameters could accurately describe variation in colonization. However, upon further reflection, this equation was deemed to not capture enough of the factors which can influence colonization. The next attempt,

$$\frac{dM}{dt} = \frac{\frac{dF}{dt}}{\frac{dF}{dt} + g} \cdot u \cdot p, \tag{3.9}$$

included the term for the fraction of patches currently occupied. The rational behind including this term was that if there are more patches occupied than there are more owls leaving patches to colonize new ones. However this equation lacked a recognition that if the fraction of patches occupied increased too much (for the sake of this example consider if $p = 1$) then there would be fewer or no patches to colonize which would instead negatively affect the colonization rate. In order to rectify this relationship the term $(1 - p)$ was included in the new equation

$$\frac{dM}{dt} = \frac{\frac{dF}{dt}}{\frac{dF}{dt} + g} \cdot u \cdot p \cdot (1 - p). \tag{3.10}$$

However this equation was also missing a key component. Going back to the original attempt to include a term capturing fecundity, Eq.(3.8), it is obvious that the change in fecundity does not completely describe how the fecundity is changing the colonization rate. In other words it failed to capture the current value for fecundity. The rationale behind including fecundity stemmed from the idea that a large increase in fecundity combined with a large current fecundity value would increase colonization more than a similarly large increase in fecundity with a small current fecundity value. This is because the increase with the larger current fecundity value compounds itself. As an example consider only the $\frac{dF}{dt}$ and F terms where in both instances $\frac{dF}{dt} = 0.5$. However for the first case let us assume $F_1 = 0.1$ and $F_2 = 0.5$ for the second case. Now if we described these changes with simply the $\frac{dF}{dt}$ term both these cases would be the same. If we look at both terms however, $\frac{dF}{dt} \cdot F_1 = 0.05$ and $\frac{dF}{dt} \cdot F_2 = 0.25$. Here we capture the fact that increasing fecundity from 0.5 to 1.0 is more significant than increasing fecundity from 0.1 to 0.6. Some may argue that the relation of $\frac{dF}{dt}$ to F should influence the colonization more accurately since a larger relational increase could arguably lead to a greater increase in colonization. However this logic is incorrect in that an increase from $F = 0.5$ to $F = 1.0$ is more significant than from $F = 0.1$ to $F = 0.6$ when you consider their relation to the theoretical maximum for fecundity. In order to illustrate this further consider that this theoretical maximum is instead a perfect 100 on some scale (where the higher the number the more desirable). Now it is obvious an increase from 10 to 15 is not nearly as significant an achievement as an increase from 95 to 100. This is because the relation to the theoretical maximum is more significant than relation to the theoretical minimum in that the compounding nature of fecundity must be taken into account (this year's fecundity has a direct effect on the number of juvenile owls that will colonize more patches and in turn produce offspring even more offspring in the future).

The final equation was designed to work as a saturation function for the rate of change of the colonization rate similar to Eq.(3.4) for fecundity. The equation was determined to be

$$\frac{dM}{dt} = \frac{\frac{dF}{dt}}{\frac{dF}{dt} + g} \cdot u \cdot F \cdot p \cdot (1 - p) \tag{3.11}$$

and also has a foundation in the Hill equation (Eq. (3.5)). The two parameters, u and g, act similarly to k and L of Eq.(3.4). However, in this equation the values for the parameters are around $u = 50$ and $g = 3$. Since M has units of $\frac{1}{\text{time}}$, p has no units, F has units of $\frac{\text{number of female offspring}}{\text{number of females}}$, and $\frac{dF}{dt}$ has units of $\frac{\text{number of female offspring}}{\text{number of females}\cdot\text{time}}$ u must have units of $\frac{\text{number of females}}{\text{number of female offspring}\cdot\text{time}^2}$ and g must have units of $\frac{\text{number of female offspring}}{\text{number of females}\cdot\text{time}}$ in order for $\frac{dM}{dt}$ to have units of $\frac{1}{\text{time}^2}$. Fig. 3.3 shows the variation in the colonization rate according to the model. The appropriate range for this term, which was used to find the values for the u and g parameters, was based on Lee et al. (2012) who utilized owl data to determine a range of about 0.50 to 0.30 for the colonization rate and 0.20 to 0.05 for the extinction rate for their own simulation. Fig. 3.4 and Fig. 3.5 show how varying the values, of u and g respectively, effects the colonization rate. These graphs show that decreasing u or increasing g both have similar effects of decreasing variation in the colonization rate. The values chosen for each parameter also illustrate how changing one parameter can be seen to have comparable effects to changing the value of the other parameter.

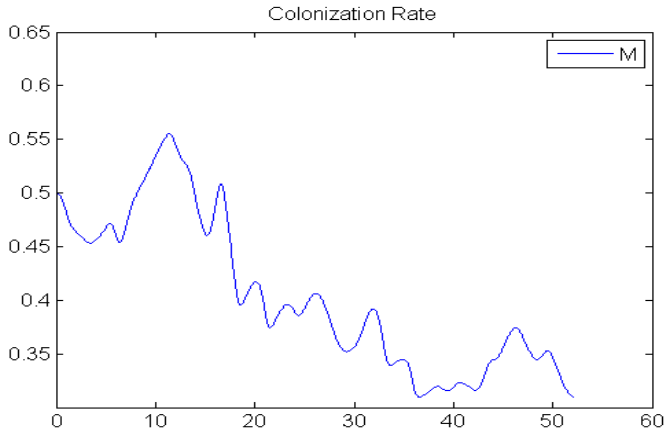

Figure 3.3: Colonization rate with respect to time ($u = 50$ and $g = 3$).

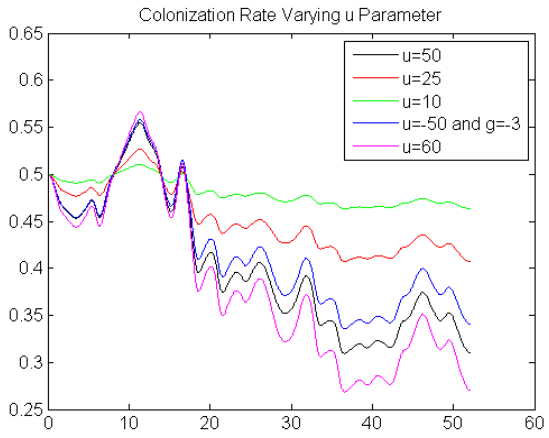

Figure 3.4: Colonization rate with varying u parameter while g parameter held constant at 3 unless specified.

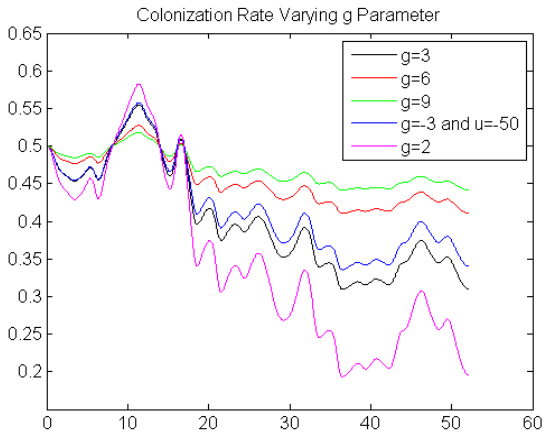

Figure 3.5: Colonization rate with varying g parameter while u parameter held constant at 50 unless specified.

Chapter 4

Results

4.1 Solving the Ordinary Differential Equations with Matlab

Matlab has eight different ordinary differential equation solvers, each of which utilizes a different method in order to solve the equation. These eight solves include: ode45, ode23, ode113, ode15s, ode23s, ode23t, ode23tb, and ode15i. The solvers are used by setting a time scale for the system to be solved and introducing a vector of initial conditions for the equations. The ode45 solver is generally the most accurate and works by utilizing an "explicit Runge-Kutta (4,5) formula, the Dormand-Prince pair" [2]. As a one-step solver, ode45 only needs the solution at the time point immediately before the one being calculated. It is best used for nonstiff problems. The ode23 solver, like ode45, is also a one-step solver. However, the ode23 solver utilizes an "explicit Runge-Kutta (2,3) pair of Bogacki and Shampine" [2]. Unlike the ode45 solver, the ode23 solver retains its viability in the presence of mild stiffness. The ode113 solver is the only solver designed for nonstiff problems which acts as a multistep solver, meaning it "needs the solutions at several preceding time points to compute the current solution" [2]. The ode113 solver is a "variable order Adams-Bashforth-Moulton PECE solver" [2]. The ode15s solver is the first of four solvers designed for stiff problems. It is a "variable-order solver based on numerical differentiation formulas while optionally using Gear's method of backward differentiation formulas" [2]. Similarly to ode113, the ode15s solver is a multistep solver. The ode23s solver is a one-step solver which utilizes a modified Rosenbrock formula of order 2 to solve stiff problems. The ode23t solver is "an implementation of the trapezoidal rule using a 'free' interpolant" [2]. This solver is best when the problem is only moderately stiff and must be solved without numerical damping. The ode23tb solver utilizes an "implementation of TR-BDF2, an implicit Runge-Kutta formula with a first stage that is trapezoidal rule step and a second stage that is backward differentiation formula of order 2" [2]. The ode15i solver is designed for fully implicit differential equations and utilizes backward differentiation formulas. For this model the ode23 solver was implemented (as shown below) due to its success with mildly stiff problems however all the solvers except ode15i could be utilized successfully. In the code shown below, the $[0, 52]$ is the time interval for which the solver is running (in this case the length of time for which rainfall data was available). The $[.922; .40, .5]$ represents the initial conditions vector where $p = 0.922$, $F = 0.40$, and $M = 0.5$. The options line of code controls both the error relative to the size of each solution component ($RelTol$) as well as the threshold near zero below which the solution component for each differential equation is unimportant ($AbsTol$).

```
options= odeset('RelTol',1e-9,'AbsTol',1e-9*ones(1,3));
[t,x] = ode23('derivRFL4',[0,52],[.922;.40;.5],options);
```

4.2 Varying Initial Conditions

4.2.1 Varying Initial Condition for Colonization Rate

The next step for the model is to observe its behavior while varying initial conditions as well as parameters. In doing so, the model demonstrates which of its components have the largest effect on the data it yields. This discussion will begin by observing the effects of altering the initial condition for colonization rate. Since the equation for fecundity depends only on the rainfall metric (and neither the fraction of patches nor the colonization rate) its behavior remains consistent and thus has been omitted from some sections. Fig. 4.1 and Fig. 4.3 both depict the fraction of patches occupied however the former demonstrates the result of dropping the initial condition for colonization rate from 0.50 to 0.30 while the latter illustrates an increase in the initial condition for colonization rate from 0.50 to 0.60. Fig. 4.2 and Fig. 4.4 portray the effect of each variation on the colonization rate's behavior.

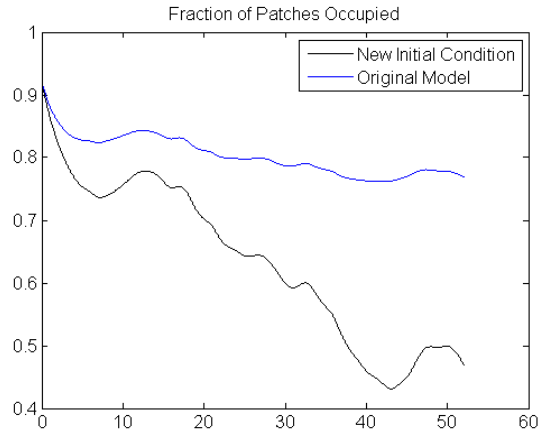

Figure 4.1: Fraction of patches occupied with colonization rate having initial condition 0.30 (Originally 0.50).

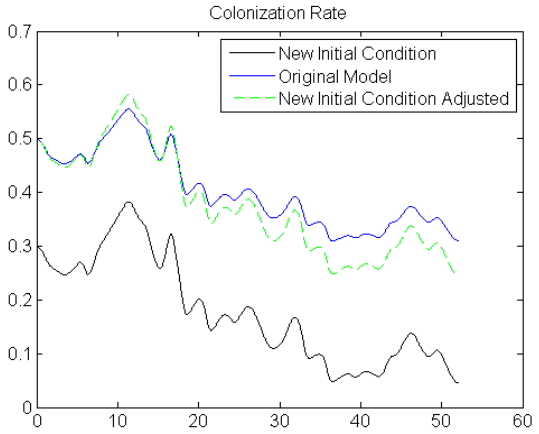

Figure 4.2: Colonization rate with initial condition 0.30 (Originally 0.50).

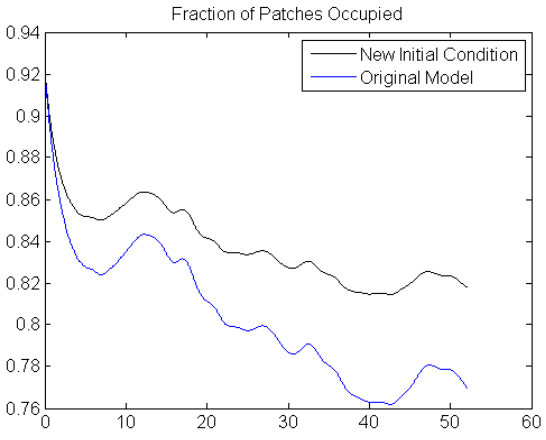

Figure 4.3: Fraction of patches occupied with colonization rate having initial condition 0.60 (Originally 0.50).

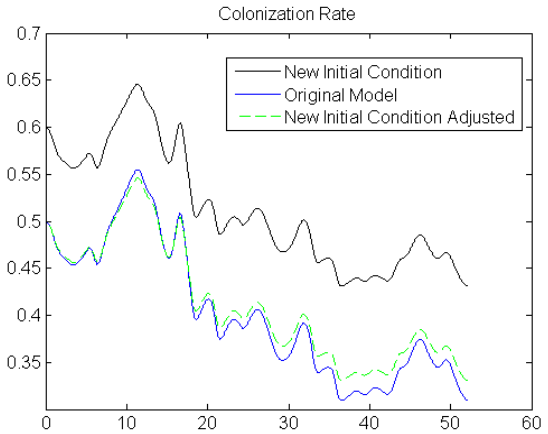

Figure 4.4: Colonization rate with initial condition 0.60 (Originally 0.50).

Although the general shape of the colonization rate curve is largely unchanged in both cases, there does appear to be deviation from the adjusted curve (the new initial condition curve shifted upward by 0.20 in Fig. 4.2 and downward by 0.10 in Fig. 4.4). This deviation is due to the fact that the change in colonization rate equation (Eq.(3.11)) incorporates both fraction of patches occupied (p) as well as a term for the fraction of patches unoccupied ($1 - p$). Therefore these terms are maximized when fraction of patches occupied is at 0.50. However the adjusted new initial condition curve in Fig. 4.2 also drops lower than the original model at around year twenty and remains lower for the rest of the time span. Alternately, Fig. 4.4 remains above the original model beginning at around year twenty. From Fig. 4.2 we can see that the adjusted new initial condition curve has larger peaks and lower valleys than the original model. The interaction between the curves in Fig. 4.2 can be aptly described by their relation to the initial condition, as whenever the curves are not at their initial condition, the new initial condition curves have a larger deviation (both higher when above the initial condition and lower when below the initial condition). Ultimately the final value for colonization rate in Fig. 4.2 is about 0.31 for the original model and 0.25 for the adjusted new initial condition curve (for Fig. 4.4 it is about 0.33 for the adjusted new initial condition curve) thus demonstrating that for every 0.10 deviation in the initial condition there is approximately a 0.02 change in the terminating value, which accounts for about 6.45% of the terminating value of the original model.

Similar to the colonization rate, which does not appear to vary greatly from a change in initial condition (aside from the higher peaks and lower valleys the general shape of the curve is consistent), Fig. 4.1 and Fig. 4.3 show the fraction of patches occupied maintains a general curve shape however the equilibrium values are altered drastically. This behavior is due to the presence of the M term which lies in Eq.(3.1). Since colonization rate in Fig. 4.2 is now consistently about 0.2 less than in the original model, it is obvious that the value for fraction of patches should also be consistently less than in the original model. The terminating values for the fraction of patches occupied are about 0.77 for the original model, 0.47 for the initial condition of 0.5 in Fig. 4.1, and 0.82 for the initial condition of 0.833 in Fig. 4.3. As such we observe a 0.30 drop in the final value for Fig. 4.1 which accounts for about 38.96% of the final value for the original model which is comparable to the 40% drop in the initial condition for colonization rate (for Fig. 4.3 there is a 0.05 increase, or 6.49% increase from the original model compared to the 10% increase in the initial condition).

4.2.2 Varying Initial Condition for Fraction of Patches

The next initial condition that was varied was the fraction of patches. The original model had the initial condition set as 0.922 while the new initial conditions were dropped to 0.50 and 0.833. The former new initial condition describes a situation where the spotted owls have a large amount of habitats available to colonize (this could be a proposal to describe how the populations would respond to having the suitable habitat amount reintroduced at a large scale). Fig. 4.5 shows how the fraction of patches responds to the new initial condition of 0.50 while Fig. 4.7 utilizes the initial condition of 0.833. The curves for the original model and the new initial condition are both similar in each case, with a tendency towards slightly different equilibriums aside from the first ten years which rapidly return the curves to their equilibriums. Fig. 4.7 was an interesting case as the initial condition was set to the equilibrium value based on the other initial conditions. The new initial condition curves for fraction of patches always have lower values than the original model however, due to the colonization rate's response to the new initial condition. The terminating values for each curve are as follows: approximately 0.77 for the original model, 0.74 for the initial conditions used in Fig. 4.5, and 0.76 for the initial conditions used in Fig. 4.5. Thus the variation in the terminating equilibrium value is comparatively small to the change in the initial condition. Fig. 4.6 and Fig. 4.8 depict the colonization

rate's new behavior. The colonization rate again has a similar shape between its original model curve and new initial condition curve. However, since the equation for rate of change of colonization rate (Eq.(3.11)) depends on both fraction of patches, p, as well as $(1-p)$ and since the colonization rate begins with a negative rate of change (due to the presence of the rate of change of fecundity term) the initial decrease is larger for the new initial conditions than for the original model. Since the overall trend of the colonization rate is negative (again due to the negative trend of fecundity) the new initial condition curve for colonization rate remains lower than the original model curve.

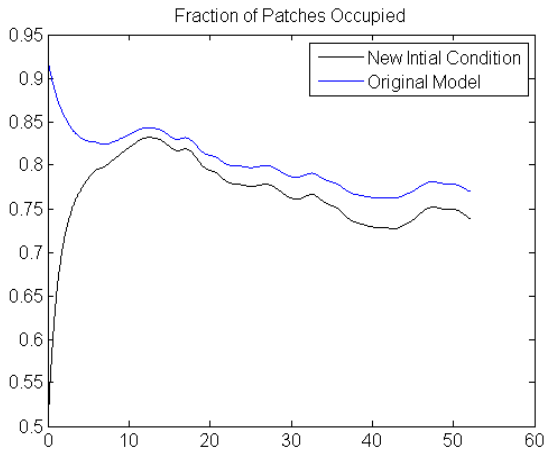

Figure 4.5: Fraction of patches occupied with initial condition 0.50 (Originally 0.922).

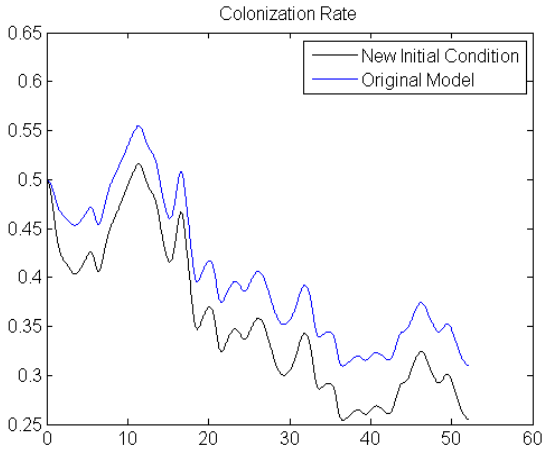

Figure 4.6: Colonization rate with fraction of patches occupied having initial condition 0.50 (Originally 0.922).

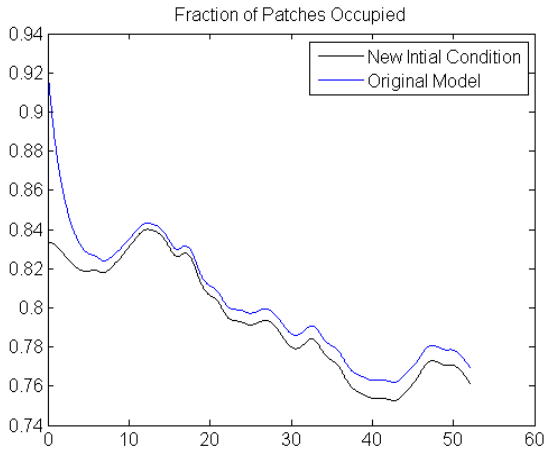

Figure 4.7: Fraction of patches occupied with initial condition 0.833 (Originally 0.922).

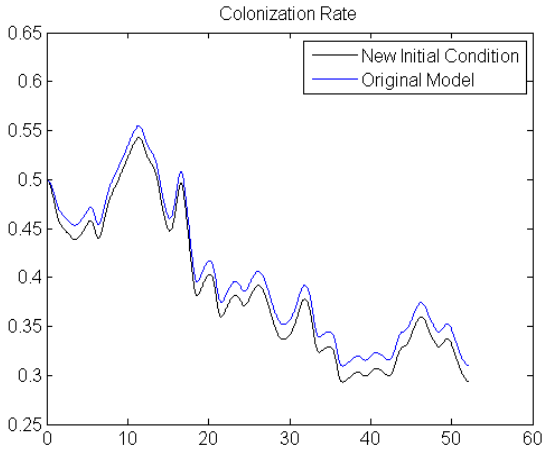

Figure 4.8: Colonization rate with fraction of patches occupied having initial condition 0.833 (Originally 0.922).

4.2.3 Varying Initial Condition for Fecundity

The final initial condition to be modified was for fecundity which was originally set to 0.50 while now dropped to 0.40. The curve for fecundity (seen in Fig. 4.9) maintained exactly the same shape

for the curve between the original model and the new initial condition with every value decreased by exactly 0.10. The effect on the colonization rate of this decrease in fecundity is depicted in Fig. 4.11. Fig. 4.11 shows decreasing the initial condition for fecundity has a similar effect on the colonization rate curve as the effect of decreasing the initial condition for colonization rate itself in that whenever the curve is below its initial value the new initial condition curve is lower than the original model (while the converse is true when the curves are above the initial value). The difference between varying the initial condition for colonization rate and fecundity is that the fecundity variation results in larger variation between the shape of the curves (and the curves of course now begin at the same initial condition). Fig. 4.10 depicts the fraction of patches occupied with the new initial condition for fecundity. Again since Eq.(3.1) depends on the colonization rate, there is symmetry between the behavior of the new initial condition colonization rate curve in relation to its original model curve and the new initial condition fraction of patches occupied curve to its original model curve.

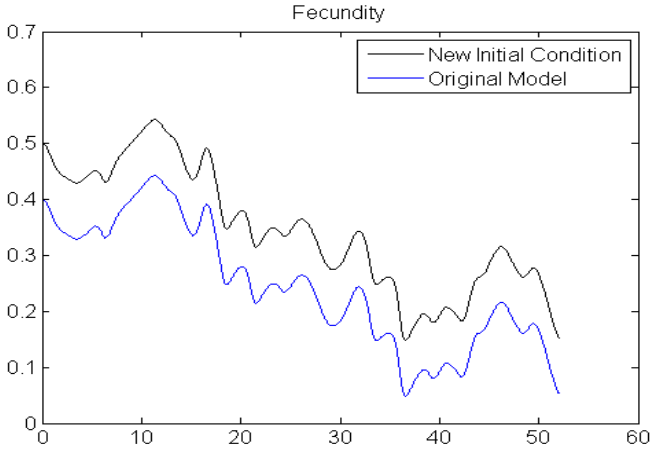

Figure 4.9: Fecundity with initial condition 0.50 (Originally 0.40).

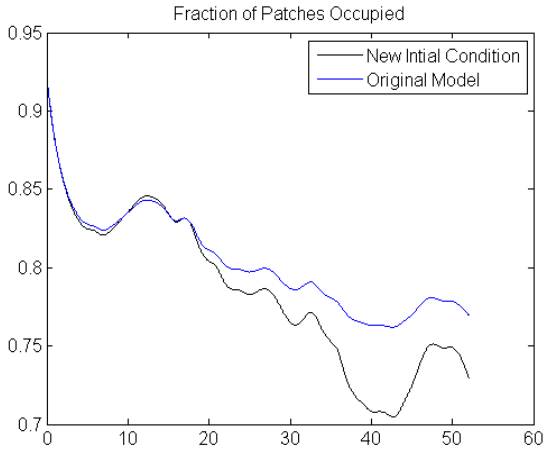

Figure 4.10: Fraction of patches occupied with fecundity having initial condition 0.50 (Originally 0.40).

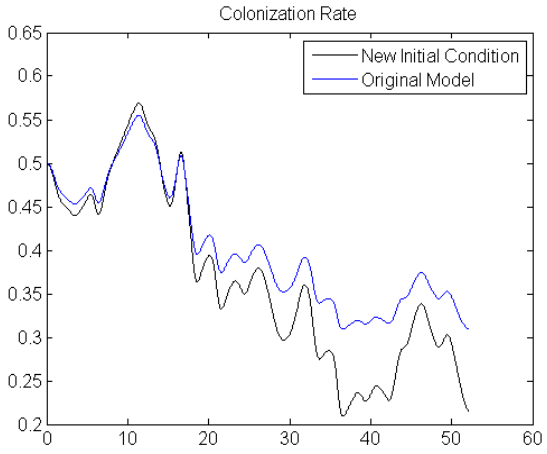

Figure 4.11: Colonization rate with fecundity having initial condition 0.50 (Originally 0.40).

In terms of terminating values, the 25% increase in fecundity (from 0.40 to 0.50) results in a decrease

in both fraction of patches occupied and colonization rate demonstrating how this is a case in which this model may not be the most accurate in predicting the behavior of the spotted owls. Since Eq. (3.11) is based on both fecundity and change in fecundity, when fecundity is larger with a similarly consistent negative pattern, then the decreases in colonization are larger. Fraction of patches is then lowered in turn by the decrease in the colonization rate. Although this particular case is not being accurately depicted (an increase in fecundity should increase the fraction of patches occupied and the colonization rate) it still accurately describes cases where fecundity does not have a constant negative trend which can be observed in this set of figures (Fig. 4.9, Fig. 4.10, and Fig. 4.11) during the first ten years.

4.3 Varying Parameters

4.3.1 Varying a Parameter

The next section will look at how altering the values of the parameters effects the curves. The first parameter under consideration will be the a parameter found in Eq.(3.1) which describes the range of the patch sizes. When a is small it represents patches which have large variation between the sizes while a large value for a represents patches of identical size. In the original model the a parameter was set to 0 since the patch sizes had large variation. Fig. 4.12 depicts the effect on the fraction of patches occupied when the a parameter is adjusted to 1.0 while Fig. 4.14 shows the result of the a parameter being set to a large value. In both cases we see the value of the fraction of patches occupied being lower than the original model, thus demonstrating how the a parameter negatively influences the fraction of patches occupied. The increase of the a parameter from 0 to 1.0 results in about a 0.02 drop in the terminating value for the fraction of patches (from 0.77 in the original model to 0.75 for the adjusted parameter curve) while the increase to a large a value resulted in a drop of about 0.08 (from 0.77 to 0.69). These drops represent respectively 2.60% and 10.39% of the terminating value of the original model. Fig. 4.13 and Fig. 4.15 show the effects of the a parameter on the colonization rate. Again the colonization rate demonstrates behavior where the adjusted parameter curve is above the original model curve when they are above the initial condition while the opposite holds true when the curves are below the initial condition. This behavior is once again due to the presence of both the p and $(1-p)$ terms in Eq.(3.11). The terminating value for the case where the a parameter is adjusted to 1 is negligibly different from the original model while the increase to a large value results in about a 0.03 drop (from 0.31 to 0.28) or about 9.68% of the original model final value.

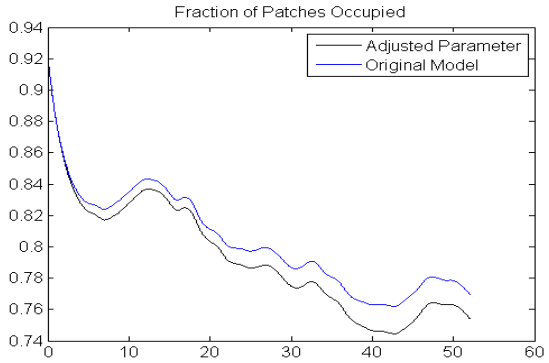

Figure 4.12: Fraction of patches occupied with a parameter set to 1.0 (Originally 0).

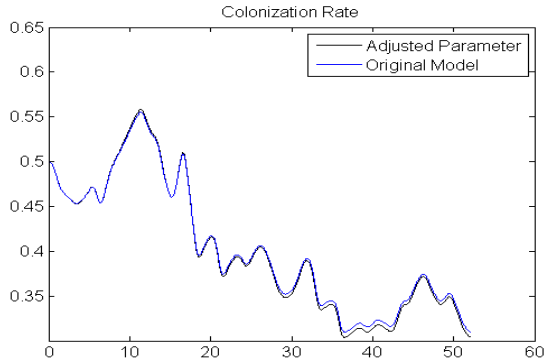

Figure 4.13: Colonization rate with a parameter set to 1.0 (Originally 0).

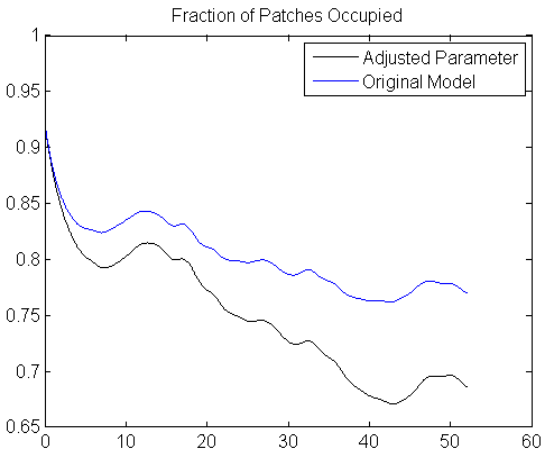

Figure 4.14: Fraction of patches occupied with large a parameter (Originally 0).

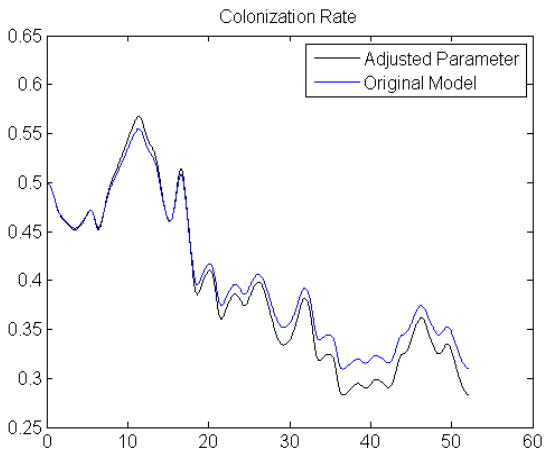

Figure 4.15: Colonization rate with large a parameter (Originally 0).

4.3.2 Varying e Parameter

The extinction rate was the next parameter to be analyzed. The extinction rate is observed in Eq.(3.1). The original value was set to 0.10 however the adjusted value of 0.20 might be more useful in protecting the spotted owls from going extinct. Looking at the pessimistic case would require more conservation effort based on the models. However, it would also be better for the owls' outlook by protecting against the possibility of the extinction rate having been underestimated. Fig. 4.16 portrays the effect of increasing the extinction rate on the fraction of patches occupied. The result is more variation in the curve (larger peaks and lower valleys) with a much lower terminal equilibrium value (now about 0.56 compared to the original of about 0.77 representing about a 27.27% drop). When looked at from the perspective of percentages the drop can be seen as small compared to the increase to the extinction rate (100% increase to the extinction rate value compared to a 27.27% decrease in fraction of patches occupied) however when looking at the ratio of the parameters the effect becomes more apparent, as an increase in extinction rate results in a 1:-2.1 drop in fraction of patches (a 0.10 increase to extinction rate resulted in a 0.21 decrease to fraction of patches). Thus we can observe that since extinction rate does not have much data currently, we may want to assume the more pessimistic cases and act accordingly in order to prevent drastic drops in the population. The other case that was considered (depicted in Fig. 4.18) was decreasing the extinction rate to 0.05. This decrease resulted in much less variation for the fraction of patches curve while also increasing the terminal equilibrium value from 0.77 to 0.89. Again we see that the ratio of the change in extinction parameter to the change in fraction of patches occupied is about 1:-2 (2.4 in this case). Fig. 4.17 and Fig. 4.19 on the other hand again depict the behavior of the colonization rate curves where the relation of the adjusted parameter curve to the original model curve depends on the curves relation to the initial condition (from the presence of the p and $(1-p)$ terms and the negative trend of the fecundity). The terminal values of these curves are as follows: 0.31 for the original model, 0.22 when extinction is set to 0.20, and 0.38 when extinction is set to 0.05. These values correspond to a 0.09 decrease (or 29.03% of the original model value) for $e = 0.20$ and a 0.07 increase (or 22.58% of the original model value) for $e = 0.05$. At first it may be counterintuitive to believe that extinction rate should effect the colonization rate however it does make sense when one considers the snowball effect from the fraction of patches occupied. For instance, a higher extinction rate means less owls surviving from year one to two and

then a lower percentage surviving from year two to three and so on leading to a much lower number of owls over time that could have been colonizing new patches.

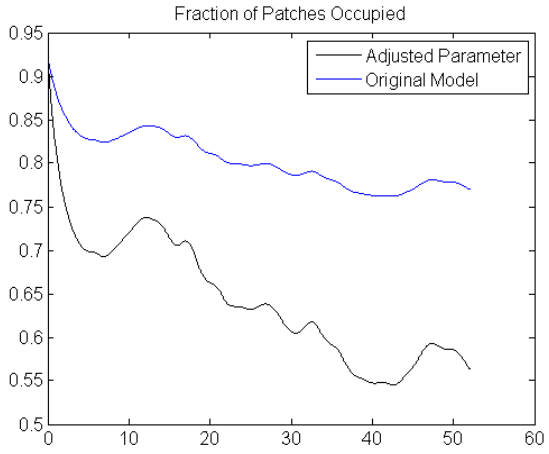

Figure 4.16: Fraction of patches occupied with extinction rate set to 0.20 (Originally 0.10).

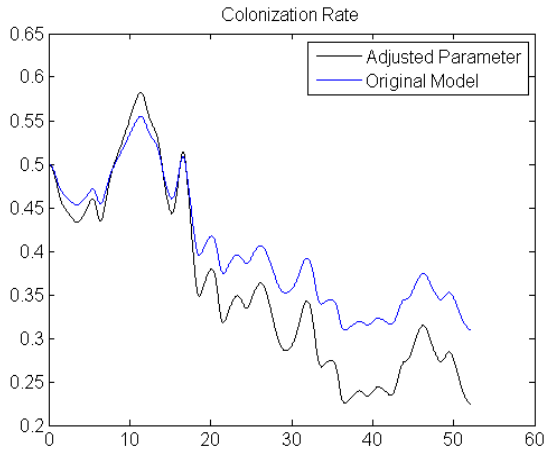

Figure 4.17: Colonization rate with extinction rate set to 0.20 (Originally 0.10).

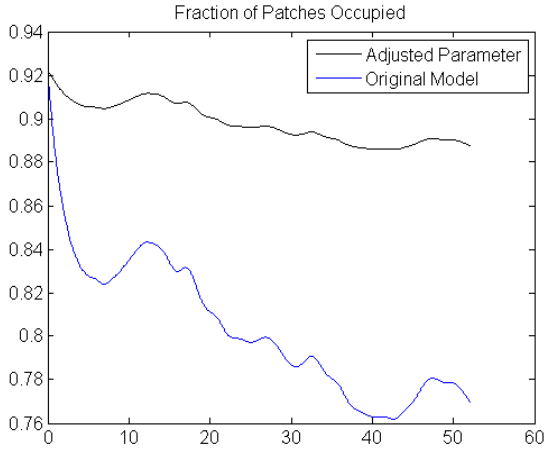

Figure 4.18: Fraction of patches occupied with extinction rate set to 0.05 (Originally 0.10).

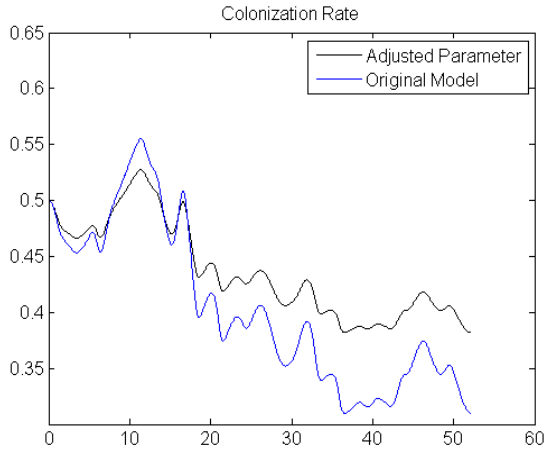

Figure 4.19: Colonization rate with extinction rate set to 0.05 (Originally 0.10).

4.3.3 Varying k and L Parameters

The next set of parameters adjusted were the k and L parameters of the rate of change of fecundity equation (Eq.(3.4)). The effect of decreasing the k parameter (from 0.20 to 0.05) yielded similar results to increasing the L parameter (from 2 to 4). In both cases the fecundity curves have been smoothed, slightly more so from the k parameter's variation than the L parameter, meaning that the value for fecundity has less deviation after the adjusted parameters (The terminal values for the fecundity figures are about 0.32 in Fig. 4.22 and 0.31 in Fig. 4.25). The result of this smoothing of the fecundity directly

translated to the colonization rate curve and then to the fraction of patches curve (illustrated in Fig. 4.22, Fig. 4.20, and Fig. 4.21 for k and Fig. 4.25, Fig. 4.23, and Fig. 4.24 for L). This is due to the presence of the term for rate of change of fecundity in Eq.(3.11) as well as the term for colonization in Eq.(3.1). They also demonstrate the expected result from higher fecundity values of increases to both fraction of patches occupied and colonization rate unlike the previous case of increasing the initial condition. The resulting equilibrium values for the adjusted parameter curves are also all higher since there is negative behavior in each of the curves which when smoothed results in less overall negative deviation. The fraction of patches curve increases from 0.77 in the original model to about 0.82 in both the figures varying k and L (representing a 6.49% increase). The ratio of the change in parameters to the change in terminal value of fraction of patches occupied is about -1:3 for k and 40:1 for L. The effects on the terminal value for colonization are also similar between the k and L figures in that the original model yields 0.31 while the k adjusted curve gives 0.43 (a 38.71% increase) and the L adjusted curve produces 0.44 (a 41.93% increase).

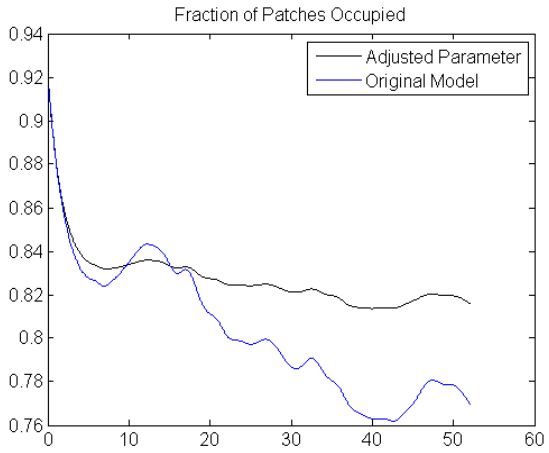

Figure 4.20: Fraction of patches occupied with k parameter set to 0.05 (Originally 0.20).

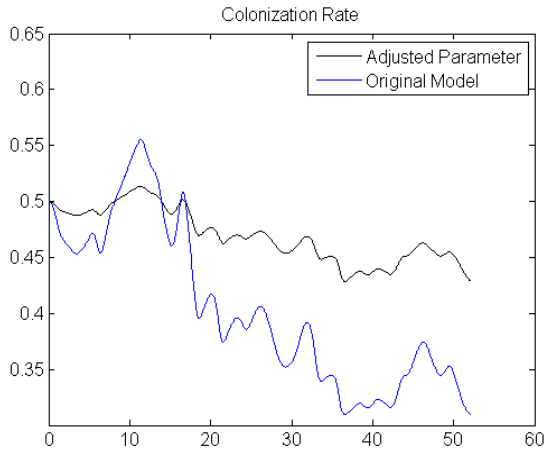

Figure 4.21: Colonization rate with k parameter set to 0.05 (Originally 0.20).

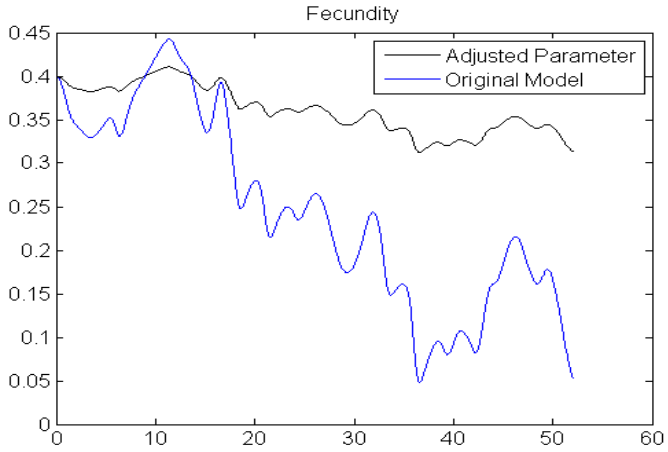

Figure 4.22: Fecundity with k parameter set to 0.05 (Originally 0.20).

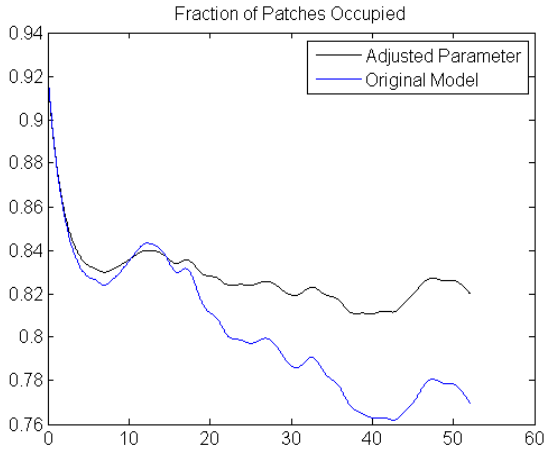

Figure 4.23: Fraction of patches occupied with L parameter set to 4 (Originally 2).

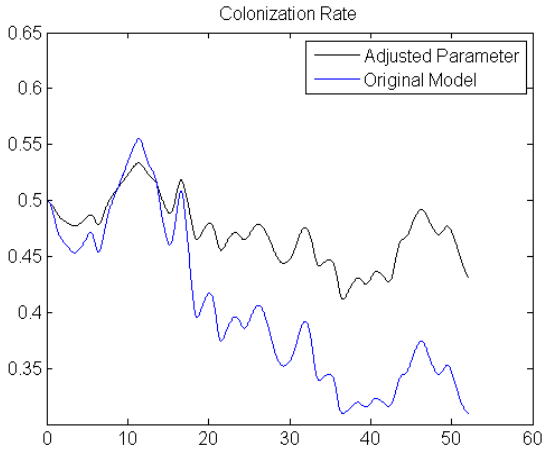

Figure 4.24: Colonization rate with L parameter set to 4 (Originally 2).

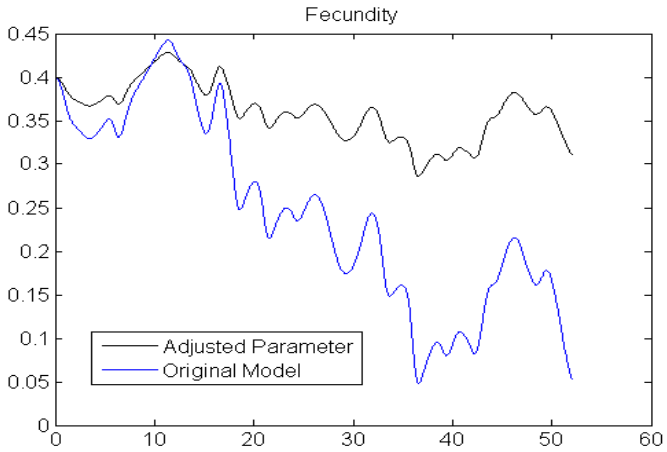

Figure 4.25: Fecundity with L parameter set to 4 (Originally 2).

4.3.4 Varying u Parameter

The next parameter which was adjusted in order to examine its effect on the model was the u parameter from Eq.(3.11). This parameter was also examined as to its effects on the colonization rate in Fig. 3.4 (however the adjusted value used in this section was not used in Fig. 3.4). The original value of u was set to be 50 while the adjusted value for this section was 75. The effect on the colonization rate is illustrated in Fig. 4.27. The result of the adjustment appears to be an increase in the variation of the colonization rate. Thus the final equilibrium value is lower for the adjusted parameter since the overall trend for the colonization rate is negative (the original model yields a terminal value of 0.31 while the adjusted parameter curve yields 0.21 corresponding to a 32.26% decrease). The ratio of the change in u parameter to the change in the terminal value of the colonization rate is 250:-1. Similarly, due to the presence of the M term in Eq.(3.1) the effect on the fraction of patches occupied is an increase in the deviation which also leads to a lower equilibrium value for the fraction of patches (the original model yields a terminal value of 0.77 while the adjusted parameter curve produces a result of 0.72 representing a 6.49% decrease) as well as a ratio of the change in u parameter to change in the

terminal value of fraction of patches occupied of 500:-1.

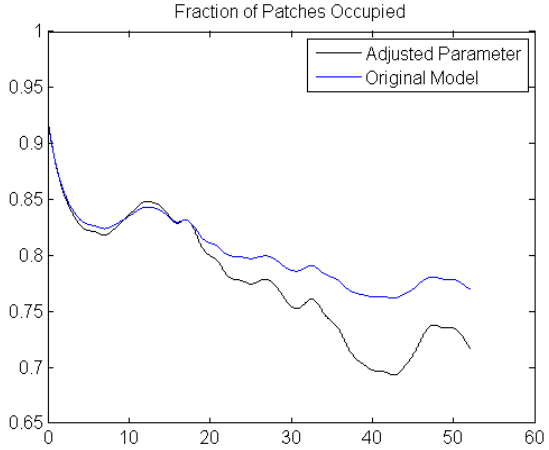

Figure 4.26: Fraction of patches occupied with u parameter set to 75 (Originally 50).

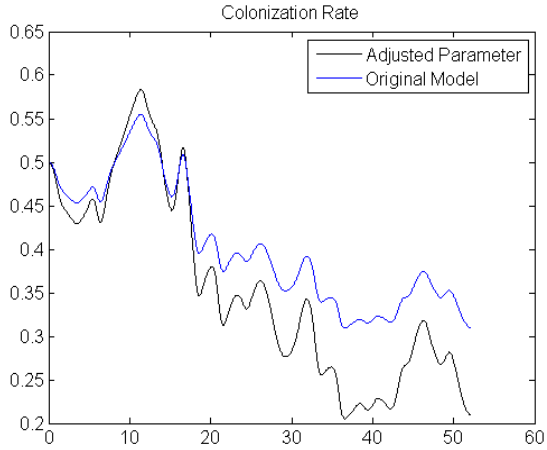

Figure 4.27: Colonization rate with u parameter set to 75 (Originally 50).

4.3.5 Varying g Parameter

The final parameter of the model to be adjusted is the g parameter of Eq.(3.11). This parameter also had its effects on colonization rate previously examined in Fig. 3.5 (however the adjusted value of 5 was not shown in this figure). The effect of increasing the g parameter had similar results as decreasing the k parameter and increasing the L parameter in that it smoothed the curves for both colonization rate and fraction of patches. Colonization rate is smoothed due to the nature of the parameter occurring in the denominator, lowering the deviation of the curve. The fraction of patches in turn is smoothed based on its dependency on the M term, as seen in Eq.(3.1). The increase of 2 to the g parameter resulted in an increase to the both terminal value of fraction of patches (0.77 for the original model curve and about 0.80 for the adjusted curve, a 3.90% increase) and the terminal value for colonization rate (0.31 for the original model curve and 0.39 for the adjusted model curve, a 25.81% increase). The ratio between the change in g parameter and the change in terminal value is about 66.66:1 for fraction of patches occupied and 25:1 for colonization rate.

Although the data appears to be realistic for all the variations, apart from the case of varying the initial condition for fecundity, there appears to be little variation in the actual behavior or the shape of the curves. These problems may be rectified by adding more equations to the model or by incorporating more data for the spotted owl which might affect the fraction of patches occupied, colonization rate, or fecundity. Some of these ideas will be explored in the Discussion chapter.

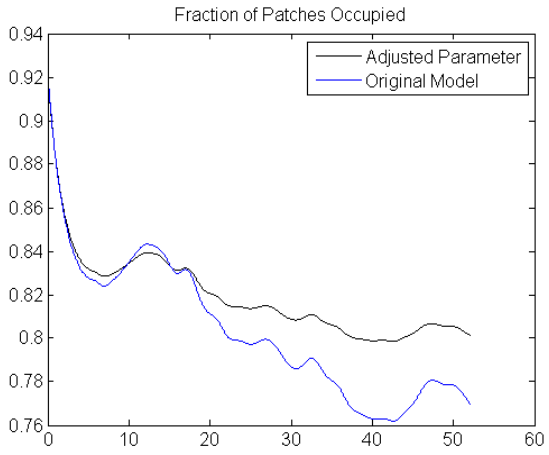

Figure 4.28: Fraction of patches occupied with g parameter set to 5 (Originally 3).

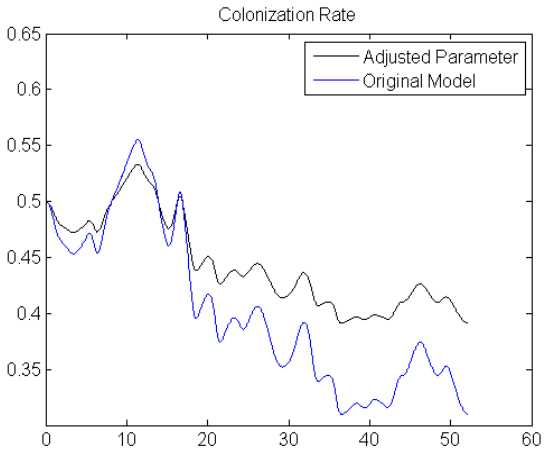

Figure 4.29: Colonization rate with g parameter set to 5 (Originally 3).

4.4 Sensitivity Analysis

4.4.1 Hanski's Modified Levins Model

Sensitivity analysis is accomplished by determining the relative sensitivity of the model's values to changes in the parameters. First the global sensitivities are established by taking the partial derivative of the model in question with respect to each parameter, almost treating them as a variable in each instance. These partial derivatives are normalized to remove the affects of units through the use of (4.5) and then analyzed where a larger value signifies that the model is more sensitive to that parameter. In addition to the strength of the parameter, the sign of the sensitivity demonstrates whether the parameter increases or decreases the output variable (where a positive sensitivity signifies that increasing the parameter increases the output variable and a negative sensitivity signifies that increasing a parameter decreases the output variable) [17]. Hanski's modified Levins model

$$\frac{dp}{dt} = \underbrace{m\left[(1+a)\frac{p}{a+p}\right](1-p)}_{A} - \underbrace{e\left[\frac{a\cdot p}{1+a}+\frac{p^2}{a+p}\right]}_{B}, \tag{4.1}$$

was analyzed first since it was used as the foundation for the fraction of patches occupied equation in the new model. Eq.(4.1) had its partial derivative taken with respect to the a, m, and e parameters respectively to produce

$$\begin{aligned}\frac{\partial}{\partial t}\left[\frac{\partial p}{\partial a}\right] = &\underbrace{m\cdot\frac{(a+p)\cdot\left[p+(1+a)\cdot\frac{\partial p}{\partial a}\right]-(1+a)\cdot p\cdot\left(1+\frac{\partial p}{\partial a}\right)}{(a+p)^2}\cdot(1-p)}_{1} - \underbrace{m\cdot\frac{(1+a)\cdot p}{a+p}\cdot\frac{\partial p}{\partial a}}_{2}\\ &\underbrace{-e\cdot\frac{(1+a)\cdot\left(p+\frac{\partial p}{\partial a}\cdot a\right)-a\cdot p}{(1+a)^2}}_{3} - \underbrace{e\cdot\frac{(a+p)\cdot 2\cdot p\cdot\frac{\partial p}{\partial a}-p^2\cdot\left(1+\frac{\partial p}{\partial a}\right)}{(a+p)^2}}_{4},\end{aligned} \tag{4.2}$$

$$\begin{aligned}\frac{\partial}{\partial t}\left[\frac{\partial p}{\partial m}\right] = &\frac{(1+a)\cdot p}{a+p}\cdot(1-p)+m\cdot\frac{(a+p)\cdot(1+a)\cdot\frac{\partial p}{\partial m}-(1+a)\cdot p\cdot\frac{\partial p}{\partial m}}{(a+p^2)}\cdot(1-p)-m\cdot\frac{(1+a)\cdot p}{a+p}\cdot\frac{\partial p}{\partial m}\\ &-\frac{e\cdot a\cdot\frac{\partial p}{\partial m}}{1+a}-\frac{(a+p)\cdot e\cdot 2\cdot p\cdot\frac{\partial p}{\partial m}-e\cdot p^2\cdot\frac{\partial p}{\partial m}}{(a+p)^2},\end{aligned} \tag{4.3}$$

$$\begin{aligned}\frac{\partial}{\partial t}\left[\frac{\partial p}{\partial e}\right] = &m\cdot\frac{(a+p)\cdot(1+a)\cdot\frac{\partial p}{\partial e}-(1+a)\cdot p\cdot\frac{\partial p}{\partial e}}{(a+p)^2}\cdot(1-p)-m\cdot\frac{(1+a)\cdot p}{a+p}\cdot\frac{\partial p}{\partial e}-\frac{a\cdot p}{1+a}-\frac{p^2}{a+p}\\ &-\frac{e\cdot a\cdot\frac{\partial p}{\partial e}}{1+a}-\frac{(a+p)\cdot e\cdot 2\cdot p\cdot\frac{\partial p}{\partial e}-e\cdot p^2\cdot\frac{\partial p}{\partial e}}{(a+p^2)},\end{aligned} \tag{4.4}$$

to consider the effects of each parameter on the model. In order to observe how these equations were developed, consider Eq.(4.1) and Eq.(4.2) which have each of their terms labeled. Terms 1 and 2 of Eq.(4.2) were the result of using the product rule on term A of Eq.(4.1) since it contained both p, a variable dependent on a, as well as the a parameter itself. Since m is not dependent on a it was

treated as a constant. The quotient rule was first utilized on $\left[(1+a)\frac{p}{a+p}\right]$ of Eq.(4.1), as according to the product rule the first part of the term has its derivative taken while the second, the $(1-p)$, is maintained. The second half of the product rule resulted in term 2, where $\left[(1+a)\frac{p}{a+p}\right]$ was now maintained while $(1-p)$ had its derivative taken. Terms 3 and 4 were the result of using the product rule on term B of Eq.(4.1) which similarly included both p and a along with the e parameter which was treated as a constant. Term 3 was the result of using the quotient rule on $\frac{a \cdot p}{1+a}$ from Eq.(4.1) while term 4 resulted from utilizing the quotient rule on $\frac{p^2}{a+p}$.

The three new differential equations, in addition to the original Eq.(4.1), results in a system of four differential equations that describe the sensitivity of Eq.(4.1) to each parameter. The relative sensitivity equation

$$RS = \frac{\partial Y}{\partial X_i} \cdot \frac{X_i}{Y} \tag{4.5}$$

(where X_i represents a parameter, Y the variable described by a function of X_i, and RS the relative sensitivity) is normalized and therefore does not allow for units (or increasing values) to influence its value, making it a more accurate depiction of how the model responds to a given parameter [17]. The relative sensitivity depicts information similarly to the sensitivity in that a larger value signifies a greater sensitivity of the output variable to a given parameter and the sign signifies whether increasing the parameter increases or decreases the output variable (where positive relative sensitivity signifies increasing the output variable and negative relative sensitivity signifies decreasing the output variable). The relative sensitivity of the a parameter was then graphed in Fig. 4.30 with varying initial conditions for the fraction of patches occupied. The initial conditions used were 0.922 (the value used in the new model analysis based on measured occupancy data), 0.8261 (the estimated equilibrium value for the fraction of patches), and 0.5 (a value much lower than the equilibrium which signifies a possible situation where new patches are reintroduced). By considering the relative sensitivities of the model to each parameter, their maximum absolute values could be compared against each other (in addition to their terminal values in which the fraction of patches occupied reaches its equilibrium) in order to determine their importance. The Hanski modified Levins model reached its equilibrium at around year ten therefore the figures in this section were truncated after this point. The relative sensitivity graphs varied their peaks depending on the initial conditions used for the fraction of patches occupied since the relative sensitivity equations depend inversely on the value of the fraction of patches occupied. On the other hand, the terminal values for the relative sensitivity and the concavity of the relative sensitivity curves for each parameter were approximately the same. However, the concavity of the 0.5 curves for the a and m parameters do switch concavity soon after reaching their maximum absolute values. Since each curve gradually reaches similar terminal values, and taking into account that the 0.5 curves' peak absolute values are the only curves which produce a peak absolute value larger than its terminal absolute value for each of these parameters, the switching of the concavity is expected.

In order to avoid the relative sensitivity from remaining constant at zero due to its structure, the a parameter was set to 1 rather than zero (as utilized in the new model) however the other two parameters were set to their values used in the new model. The relative sensitivity for the a and m parameters of the two higher initial conditions reached maximum absolute values at their end points since the initial conditions were so close to the equilibrium. Conversely the initial condition of 0.5 appeared to reach a maximum absolute value where the fraction of patches occupied began to become concave down. This behavior can be observed in Fig. 4.30 and Fig. 4.31 (which depicts the relative sensitivity of the model to the m parameter). However Fig. 4.32, which portrays the relative sensitivity of the model to the e parameter, shows all three initial conditions having similar behavior. Thus it would appear that the a and m parameters effects on the model is dependent on the initial condition while the

effect of the e parameter on the model seems to be independent of the initial condition. The terminal values for the relative sensitivity of each parameter were about -0.01, 0.23, and -0.16 and the maximum absolute values for the initial condition of 0.5 (since the other two initial conditions reached maximum absolute values at their terminal values) were about 0.04, 0.4, and 0.16 for the a, m, and e parameters respectively. Thus both of these sets of values show that the most to least impactful parameter is as follows: m, e, a. This behavior supports the construction of the new model to incorporate the m parameter as a function since it has the largest effect on the fraction of patches.

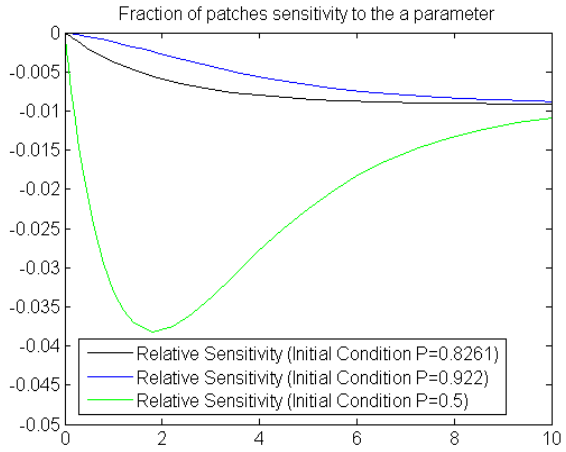

Figure 4.30: Fraction of patches occupied relative sensitivity to the a parameter for Eq.(4.1) with varying initial conditions.

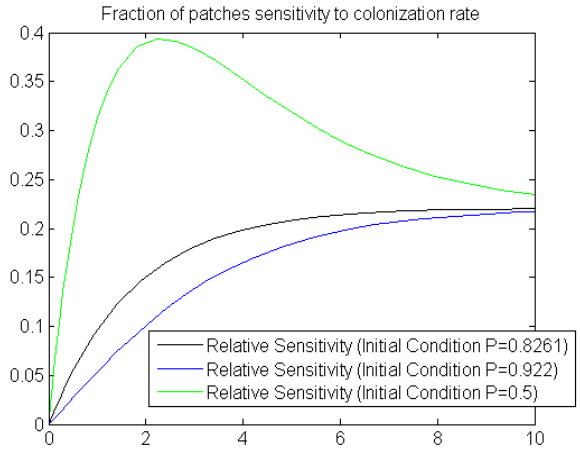

Figure 4.31: Fraction of patches occupied relative sensitivity to the colonization rate for Eq.(4.1) with varying initial conditions.

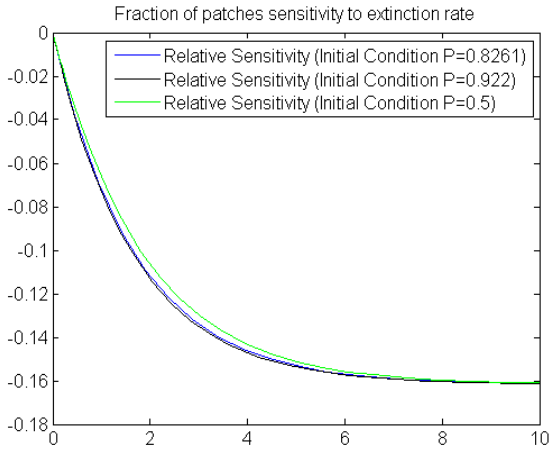

Figure 4.32: Fraction of patches occupied relative sensitivity to the extinction rate for Eq.(4.1) with varying initial conditions.

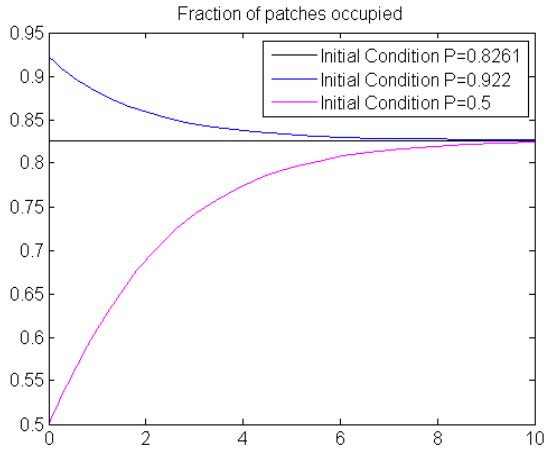

Figure 4.33: Fraction of patches occupied with respect to time for Eq.(4.1) with varying initial conditions.

4.4.2 Coupled Model

This section will now look at the sensitivity of the new model's three differential equations with respect to each parameter, demonstrating each parameters significance with regards to the predictive

values generated. Together these equations now combine to produce a set of seventeen differential equations. Similar to the section which focused on Hanski's modified Levins model, this analysis will truncate the data, however this truncation is now due to the fact that the rainfall metric needed to be held constant (at values of 1.0, 0.5, and -0.5) in order to prevent it's variations from effecting the relative sensitivities of the model to each parameter. Since the rainfall metric was held constant we will only consider the sensitivity of the model for five years at this constant value, ensuring that the values for fraction of patches occupied, fecundity, and colonization rate remained in realistic ranges and since the likelihood of having the same rainfall metric for consecutive years is not high. Fig. 4.34, Fig. 4.35, and Fig. 4.36 depict the results of the model for the fraction of patches, fecundity, and the colonization rate respectively when holding the rainfall metric constant. Although the colonization rate becomes high for the positive constant rainfall metrics, its remains in a range that could possibly occur. When analyzing Fig. 4.36, the relationship between colonization and fecundity (which due to the constant high levels of rainfall is increasingly positive) must be considered in order to recognize that this result is the product of several consecutive years of high fecundity which would create an influx of juveniles who would be searching for new patches. Thus the high colonization rates are sensible for these circumstances.

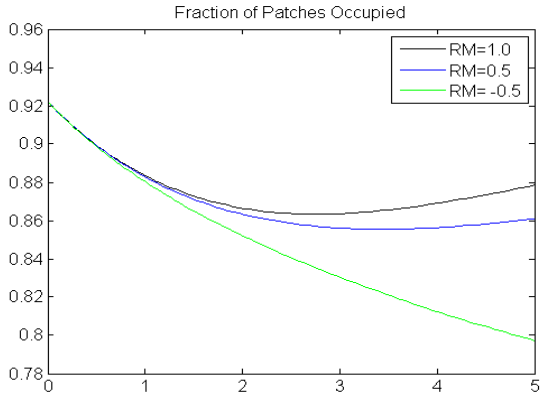

Figure 4.34: Fraction of patches occupied with respect to time with constant rainfall metrics.

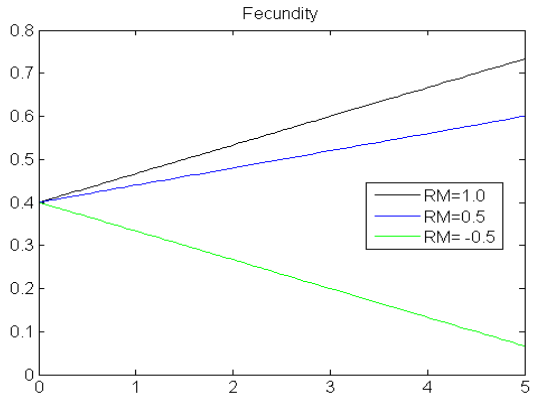

Figure 4.35: Fecundity with respect to time with constant rainfall metrics.

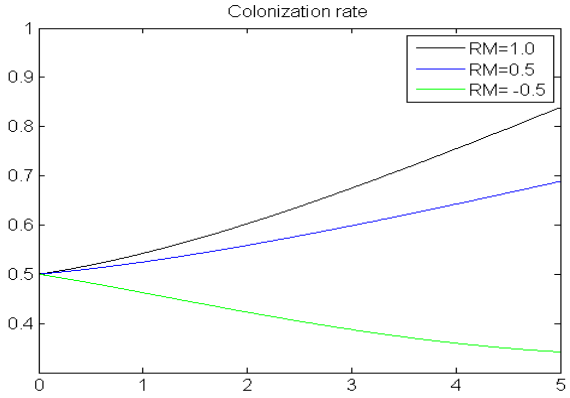

Figure 4.36: Colonization rate with respect to time with constant rainfall metrics.

The first set of equations developed from

$$\frac{dp}{dt} = M\left[(1+a)\frac{p}{a+p}\right](1-p) - e\left[\frac{a}{1+a} + \frac{p}{a+p}\right]p \tag{4.6}$$

are

$$\frac{\partial}{\partial t}\left[\frac{\partial p}{\partial a}\right] = \frac{\partial M}{\partial a}\cdot\frac{(1+a)\cdot p}{a+p}\cdot(1-p) + M\cdot\frac{(a+p)\cdot\left[(1+a)\cdot\frac{\partial p}{\partial a}+p\right] - (1+a)\cdot p\cdot\left(1+\frac{\partial p}{\partial a}\right)}{(a+p)^2}\cdot(1-p)$$
$$-M\cdot\frac{(1+a)\cdot p}{a+p}\cdot\frac{\partial p}{\partial a} - \frac{(1+a)\cdot e\cdot\left(p+\frac{\partial p}{\partial a}\cdot a\right) - e\cdot a\cdot p}{(1+a)^2} - \frac{(a+p)\cdot e\cdot 2\cdot p\cdot\frac{\partial p}{\partial a} - e\cdot p^2\cdot\left(1+\frac{\partial p}{\partial a}\right)}{(a+p)^2}, \tag{4.7}$$

$$\frac{\partial}{\partial t}\left[\frac{\partial p}{\partial e}\right] = \frac{\partial M}{\partial e}\cdot\frac{(1+a)\cdot p}{a+p}\cdot(1-p) + M\cdot\frac{(a+p)\cdot(1+a)\cdot\frac{\partial p}{\partial e} - (1+a)\cdot p\cdot\frac{\partial p}{\partial e}}{(a+p)^2}\cdot(1-p)$$
$$-M\cdot\frac{(1+a)\cdot p}{a+p}\cdot\frac{\partial p}{\partial e} - \frac{(1+a)\cdot\left(p+\frac{\partial p}{\partial e}\cdot e\right)\cdot a}{(1+a)^2} - \frac{\left(p^2+e\cdot 2\cdot p\cdot\frac{\partial p}{\partial e}\right)\cdot(a+p) - e\cdot p^2\cdot\frac{\partial p}{\partial e}}{(a+p)^2}, \tag{4.8}$$

$$\frac{\partial}{\partial t}\left[\frac{\partial p}{\partial u}\right] = \frac{\partial M}{\partial u}\cdot\frac{(1+a)\cdot p}{a+p}\cdot(1-p) + M\cdot\frac{(a+p)\cdot(1+a)\cdot\frac{\partial p}{\partial u} - (1+a)\cdot p\cdot\frac{\partial p}{\partial u}}{(a+p)^2}\cdot(1-p)$$
$$-M\cdot\frac{(1+a)\cdot p}{a+p}\cdot\frac{\partial p}{\partial u} - \frac{e\cdot a\cdot\frac{\partial p}{\partial u}}{1+a} - \frac{(a+p)\cdot e\cdot 2\cdot p\cdot\frac{\partial p}{\partial u} - e\cdot p^2\cdot\frac{\partial p}{\partial u}}{(a+p)^2}, \tag{4.9}$$

$$\frac{\partial}{\partial t}\left[\frac{\partial p}{\partial g}\right] = \frac{\partial M}{\partial g}\cdot\frac{(1+a)\cdot p}{a+p}\cdot(1-p) + M\cdot\frac{(a+p)\cdot(1+a)\cdot\frac{\partial p}{\partial g} - (1+a)\cdot p\cdot\frac{\partial p}{\partial g}}{(a+p)^2}\cdot(1-p)$$
$$-M\cdot\frac{(1+a)\cdot p}{a+p}\cdot\frac{\partial p}{\partial g} - \frac{e\cdot a\cdot\frac{\partial p}{\partial g}}{1+a} - \frac{(a+p)\cdot e\cdot 2\cdot p\cdot\frac{\partial p}{\partial g} - e\cdot p^2\cdot\frac{\partial p}{\partial g}}{(a+p)^2}, \tag{4.10}$$

$$\frac{\partial}{\partial t}\left[\frac{\partial p}{\partial k}\right] = \frac{\partial M}{\partial k}\cdot\frac{(1+a)\cdot p}{a+p}\cdot(1-p) + M\cdot\frac{(a+p)\cdot(1+a)\cdot\frac{\partial p}{\partial k} - (1+a)\cdot p\cdot\frac{\partial p}{\partial k}}{(a+p)^2}\cdot(1-p)$$
$$-M\cdot\frac{(1+a)\cdot p}{a+p}\cdot\frac{\partial p}{\partial k} - \frac{e\cdot a\cdot\frac{\partial p}{\partial k}}{1+a} - \frac{(a+p)\cdot e\cdot 2\cdot p\cdot\frac{\partial p}{\partial k} - e\cdot p^2\cdot\frac{\partial p}{\partial k}}{(a+p)^2}, \tag{4.11}$$

$$\frac{\partial}{\partial t}\left[\frac{\partial p}{\partial k}\right] = \frac{\partial M}{\partial L}\cdot\frac{(1+a)\cdot p}{a+p}\cdot(1-p) + M\cdot\frac{(a+p)\cdot(1+a)\cdot\frac{\partial p}{\partial L} - (1+a)\cdot p\cdot\frac{\partial p}{\partial L}}{(a+p)^2}\cdot(1-p)$$
$$-M\cdot\frac{(1+a)\cdot p}{a+p}\cdot\frac{\partial p}{\partial L} - \frac{e\cdot a\cdot\frac{\partial p}{\partial L}}{1+a} - \frac{(a+p)\cdot e\cdot 2\cdot p\cdot\frac{\partial p}{\partial L} - e\cdot p^2\cdot\frac{\partial p}{\partial L}}{(a+p)^2}, \tag{4.12}$$

in which Eq.(4.6) was differentiated with respect to the a, e, u, g, k, and L parameters. The results of the relative sensitivity of fraction of patches occupied with respect to the a parameter were graphed in Fig. 4.37 for the five year period. Although it is hard to detect from the figure, the relative sensitivity

became negative for all three rainfall metrics utilized. The maximum absolute value of the curves are 0.0042, 0.0050, and 0.0085 for the rainfall metrics of 1.0, 0.5, and -0.5 respectively. However compared to all the other parameters, the a parameter had minimal effects on the fraction of patches occupied. The relative sensitivity of Eq.(4.6) to the e parameter was graphed in Fig. 4.38. The effect of the e parameter on Eq.(4.6) is much more apparent than the a parameter as the curves no longer appear to remain constant at zero. Again, all three rainfall metrics utilized result in negative relative sensitivities, however there is now also a notable difference between the positive rainfall metric curves and the negative rainfall metric curve. The maximum absolute values for the relative sensitivity curves are 0.1196, 0.1323, and 0.2345 for the rainfall metrics of 1.0, 0.5, and -0.5 respectively. These maximal absolute values show a similar pattern to the a parameter's (albeit at a much larger scale) in which the lower the rainfall metric, the larger the maximal absolute value of the relative sensitivity. The relative sensitivity curves for the e parameter also appear to be concave up.

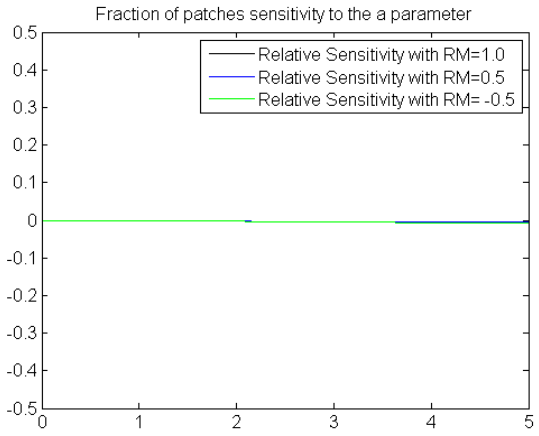

Figure 4.37: Fraction of patches occupied relative sensitivity to the a parameter with constant rainfall metrics.

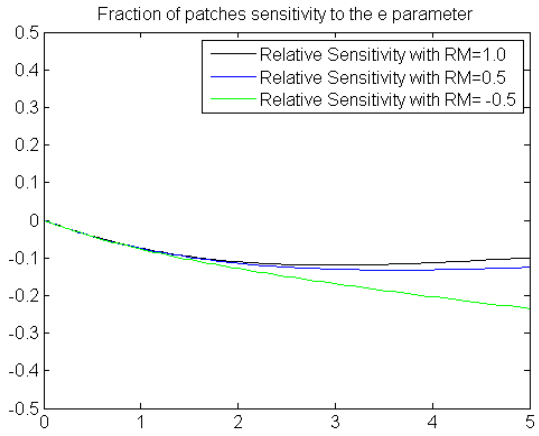

Figure 4.38: Fraction of patches occupied relative sensitivity to the e parameter with constant rainfall metrics.

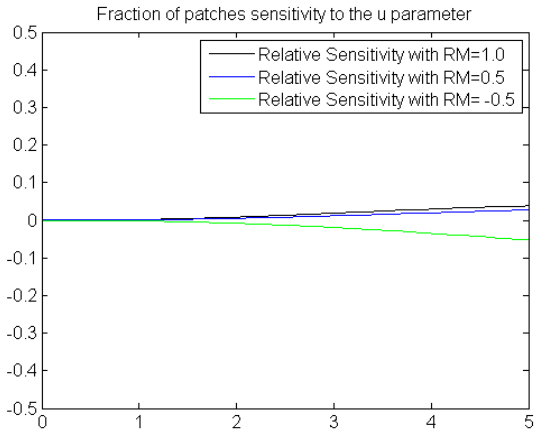

Figure 4.39: Fraction of patches occupied relative sensitivity to the u parameter with constant rainfall metrics.

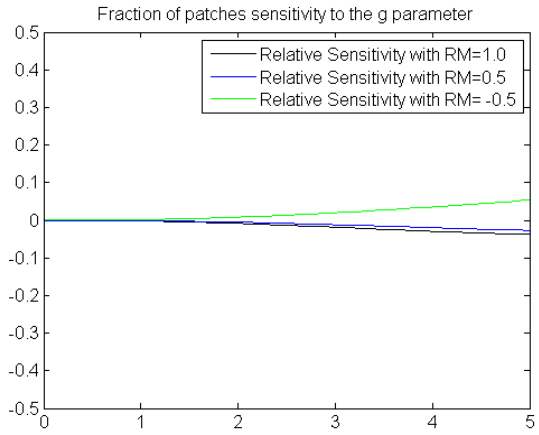

Figure 4.40: Fraction of patches occupied relative sensitivity to the g parameter with constant rainfall metrics.

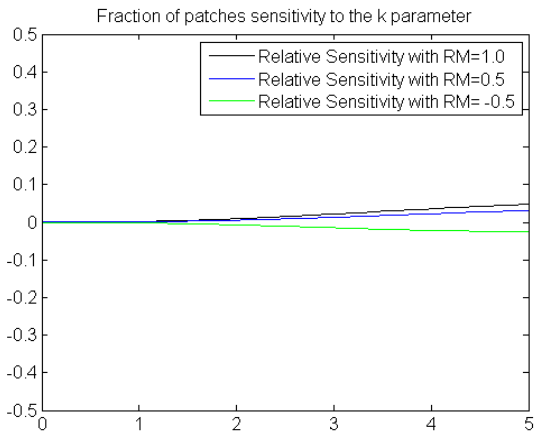

Figure 4.41: Fraction of patches occupied relative sensitivity to the k parameter with constant rainfall metrics.

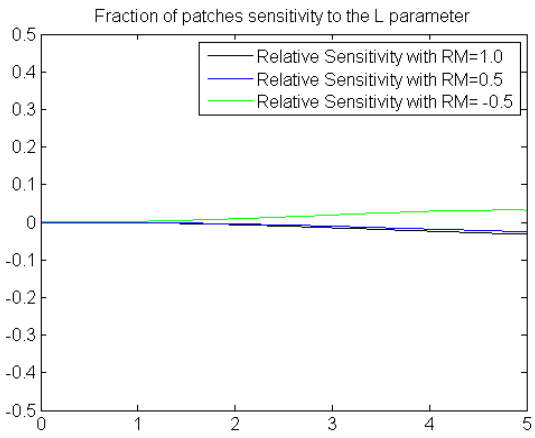

Figure 4.42: Fraction of patches occupied relative sensitivity to the L parameter with constant rainfall metrics.

Fig. 4.39 shows the relative sensitivity curves for the u parameter. These curves are the first in which the rainfall metric chosen determines the sign of the relative sensitivity. The positive rainfall metric curves resulted in positive relative sensitivities while the negative rainfall metric yielded negative relative sensitivity. The maximal absolute values for the curves are 0.0382, 0.0274, and 0.0526 for the rainfall metrics of 1.0, 0.5, and -0.5 respectively. These values do not have a consistent pattern over the jump in the change in sign of the rainfall metric (due to the sign of the rainfall metric determining the sign of the relative sensitivity). However, it does appear that negative rainfall metrics result in higher maximal absolute values for the relative sensitivity curves but as the rainfall metric approaches zero from both directions, the relative sensitivity curves maximal absolute values decrease. The relative sensitivities of Eq.(4.6) with respect to the g parameter for the rainfall metrics utilized are depicted in Fig. 4.40. These curves are similar to the relative sensitivities of the u parameter after being reflected over the x-axis. In this case, the sign of the relative sensitivity curve is opposite to the sign of the rainfall metric utilized. The similarities between the relative sensitivity curves of the u and g parameters extends to the maximal absolute values of the curves in which the g parameter relative sensitivities are 0.0374, 0.0271, and 0.0538 for the rainfall metrics of 1.0, 0.5, and -0.5 respectively. Fig. 4.41 illustrates the relative sensitivities curves for the k parameter. The maximal absolute values for these curves are 0.0477, 0.0320, and 0.0242 for the rainfall metrics of 1.0, 0.5 and -0.5 respectively. The signs of the curves are similar to the u parameter's relative sensitivity curves in which the sign of the rainfall metric carried over to the sign of the relative sensitivity curve. The maximal absolute values display behavior contrary to that of the u parameter however in that the lower the rainfall metric, the lower the maximal absolute value. The L parameter's relative sensitivity curves were graphed in Fig. 4.42. This graph shows behavior resembling the g parameter in that the sign of the relative sensitivity opposes the sign of the rainfall metric utilized. At first glance it might appear as though the L parameter has a similar relation to the k parameter as the relation between the u and g parameters, however the maximal absolute values of these curves are 0.0318, 0.0256, and 0.0323 for the rainfall metrics of 1.0, 0.5 and -0.5 respectively which do not match up nearly as symmetrically to the k values as the u and g values did to each other. Now that we have all the maximal absolute values for the relative sensitivity curves for each parameter, they may be compared against each other in order to determine which the order of significance of the parameters on Eq.(4.6). From most significant parameter to least significant parameter when utilizing a positive rainfall metric we have: e, k, u, g, L, and a while for the negative

rainfall metric we have: e, g, u, L, k, and a. Thus it appears as though the rainfall metric effects the significance of the parameters since they all have comparatively similar maximal absolute values aside from the e and a parameters, which are the most and least significant parameters respectively.

The next set of equations developed from

$$\frac{dF}{dt} = \frac{k \cdot RM}{RM + L} \tag{4.13}$$

are

$$\frac{\partial}{\partial t}\left[\frac{\partial F}{\partial k}\right] = \frac{RM}{RM + L}, \tag{4.14}$$

$$\frac{\partial}{\partial t}\left[\frac{\partial F}{\partial L}\right] = \frac{-k \cdot RM}{(RM + L)^2}, \tag{4.15}$$

in which Eq.(4.13) was differentiated with respect to the k and L parameters. Both these parameters produced similar yet opposite behavior in their relative sensitivity curves found in Fig. 4.43 and Fig. 4.44, for the k and L parameters respectively. For the k parameter, the sign of the relative sensitivity curve was consistent with the sign of the rainfall metric while the L parameter's relative sensitivity curves produced the opposite results. However, for both curves it is evident that the negative rainfall metric produced a much larger maximal absolute value than the positive rainfall metrics. The maximal absolute values for the k parameter are 0.4545, 0.3333, and 5.0000 while for the L parameter they are 0.3030, 0.2667, and 6.6667 (both for the rainfall metrics of 1.0, 0.5, and -0.5 respectively). Thus it would appear that both parameters have sensitivities that decrease as the rainfall metric tends towards zero. However, unlike the significance of the parameters that effect Eq.(4.6), these parameters are consistent in significance amongst all rainfall metrics. The L parameter is the most significant while the k parameter is the least. These maximal absolute values are also notably higher, for all the rainfall metrics, than all the relative sensitivity absolute maximal values for Eq.(4.6). However the biggest concern that arises from the relative sensitivities of the negative rainfall metric curves is that for periods of consistently negative rainfall metric, this model does not appear to be accurate. Thus it would appear that this model is better suited to short periods of consistently negative rainfall metric, an observation which carries over from the results discussed in the previous chapter.

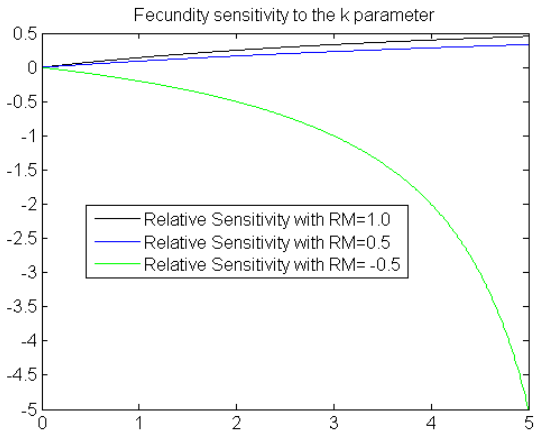

Figure 4.43: Fecundity relative sensitivity to the k parameter with constant rainfall metrics.

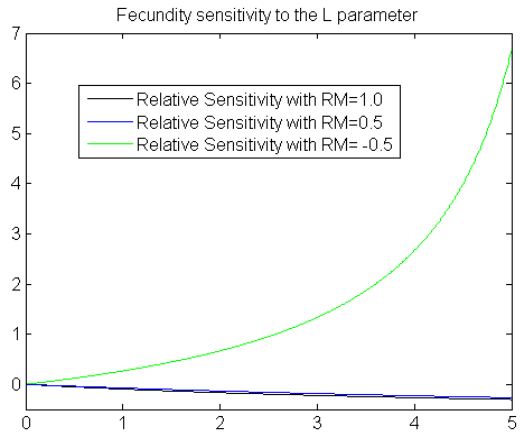

Figure 4.44: Fecundity relative sensitivity to the L parameter with constant rainfall metrics.

The final set of equations which were developed from

$$\frac{dM}{dt} = \frac{\frac{dF}{dt}}{\frac{dF}{dt} + g} \cdot u \cdot F \cdot p \cdot (1 - p) \tag{4.16}$$

are

$$\frac{\partial}{\partial t}\left[\frac{\partial M}{\partial a}\right] = \frac{u \cdot F \cdot \frac{\partial F}{\partial t} \cdot \left(\frac{\partial p}{\partial a} - 2 \cdot p \cdot \frac{\partial p}{\partial a}\right)}{\frac{\partial F}{\partial t} + g}, \tag{4.17}$$

$$\frac{\partial}{\partial t}\left[\frac{\partial M}{\partial e}\right] = \frac{u \cdot F \cdot \frac{\partial F}{\partial t} \cdot \left(\frac{\partial p}{\partial e} - 2 \cdot p \cdot \frac{\partial p}{\partial e}\right)}{\frac{\partial F}{\partial t} + g}, \tag{4.18}$$

$$\frac{\partial}{\partial t}\left[\frac{\partial M}{\partial u}\right] = \frac{F \cdot \frac{\partial F}{\partial t} \cdot (p - p^2)}{\frac{\partial F}{\partial t} + g} + \frac{u \cdot F \cdot \frac{\partial F}{\partial t} \cdot (\frac{\partial p}{\partial u} - 2 \cdot p \cdot \frac{\partial p}{\partial u})}{\frac{\partial F}{\partial t} + g}, \tag{4.19}$$

$$\frac{\partial}{\partial t}\left[\frac{\partial M}{\partial g}\right] = \frac{u \cdot F \cdot \frac{\partial F}{\partial t} \cdot \left(\frac{\partial F}{\partial t} + g\right) \cdot \left(\frac{\partial p}{\partial g} - 2 \cdot p \cdot \frac{\partial p}{\partial g}\right) - u \cdot F \cdot \frac{\partial F}{\partial t} \cdot (p - p^2)}{\left(\frac{\partial F}{\partial t} + g\right)^2}, \tag{4.20}$$

$$\begin{aligned}\frac{\partial}{\partial t}\left[\frac{\partial M}{\partial k}\right] = {} & \frac{\left(\frac{\partial F}{\partial t} + g\right) \cdot u \cdot \left[\frac{\partial F}{\partial k} \cdot \frac{\partial F}{\partial t} \cdot (p - p^2) + F \cdot \frac{\partial}{\partial t}\frac{\partial F}{\partial k} \cdot (p - p^2) + F \cdot \frac{\partial F}{\partial t} \cdot \left(\frac{\partial p}{\partial k} - 2 \cdot p \cdot \frac{\partial p}{\partial k}\right)\right]}{\left(\frac{\partial F}{\partial t} + g\right)^2} \\ & - \frac{u \cdot F \cdot \frac{\partial F}{\partial t} \cdot (p - p^2) \cdot \frac{\partial}{\partial t}\frac{\partial F}{\partial k}}{\left(\frac{\partial F}{\partial t} + g\right)^2},\end{aligned} \tag{4.21}$$

$$\begin{aligned}\frac{\partial}{\partial t}\left[\frac{\partial M}{\partial L}\right] = {} & \frac{\left(\frac{\partial F}{\partial t} + g\right) \cdot u \cdot \left[\frac{\partial F}{\partial L} \cdot \frac{\partial F}{\partial t} \cdot (p - p^2) + F \cdot \frac{\partial}{\partial t}\frac{\partial F}{\partial L} \cdot (p - p^2) + F \cdot \frac{\partial F}{\partial t} \cdot \left(\frac{\partial p}{\partial L} - 2 \cdot p \cdot \frac{\partial p}{\partial L}\right)\right]}{\left(\frac{\partial F}{\partial t} + g\right)^2} \\ & - \frac{u \cdot F \cdot \frac{\partial F}{\partial t} \cdot (p - p^2) \cdot \frac{\partial}{\partial t}\frac{\partial F}{\partial L}}{\left(\frac{\partial F}{\partial t} + g\right)^2},\end{aligned} \tag{4.22}$$

in which Eq.(4.16) was differentiated with respect to the a, e, u, g, k, and L parameters. Similar to the relative sensitivity curves from Fig. 4.37, the curves in Fig. 4.45 for the a parameter do not display much variation from zero compared to the other parameters. The maximal absolute values of the curves are 0.0071, 0.0048, and 0.0061 for the rainfall metrics of 1.0, 0.5, and -0.5 respectively. The biggest difference between these curves and the curves in Fig. 4.37 is that the sign of the curves is no longer universally negative and instead is consistent with the sign of the rainfall metric. Fig. 4.46 depicts the sensitivity of Eq.(4.16) with respect to the e parameter. Again, the sign of these curves is consistent with the sign of the rainfall metric. The maximal absolute values of the curves are 0.2346, 0.1611, and 0.2550 for the rainfall metrics of 1.0, 0.5, and -0.5 respectively. Eq.(4.16) appears to have larger sensitivity to the e parameter when a negative rainfall metric is used, however the magnitude of the relative sensitivity appears to decreases as the rainfall metric tends towards zero from both directions. The u parameter was the next whose relative sensitivity was considered and graphed in Fig. 4.47. The sign of the curve, once again, is consistent with the sign of the rainfall metric. The maximal absolute values of the curves are 0.3620, 0.2577, and 0.4853 for the rainfall metric values of 1.0, 0.5, and -0.5 respectively. These curves display behavior comparable to that of the relative sensitivity curves with

regards to the e parameter. Fig. 4.48 illustrates the relative sensitivity curves for the g parameter. This is the first parameter that has the sign for the relative sensitivity opposite of the sign of the rainfall metric used. The maximal absolute values for these curves are 0.3541, 0.2543, and 0.4963. This behavior is again very similar to reflecting the curves for the u parameter over the x-axis, as was the case when analyzing the relative sensitivities of Eq.(4.6). Fig. 4.49 portrays the relative sensitivity curves for the k parameter. These curves, like the a, e, and u parameters, are consistent with the sign of the rainfall metric utilized. The maximal absolute values for the relative sensitivity curves are 0.4672, 0.3093, and 0.1982 for the rainfall metrics of 1.0, 0.5, and -0.5 respectively. However, unlike the previous parameter's relative sensitivity curves, in this case the values for the relative sensitivity appear to be lower for the negative rainfall metric. There also appears to be a linear increase to the relative sensitivities of the positive rainfall metrics while there is a concave up curve for the negative rainfall metric. Fig. 4.50 displays the relative sensitivity curves for the L parameter which at first glance may appear to be a reflection of the k parameter curves over the x-axis. However, the difference between the positive rainfall metrics maximal absolute values is much smaller in this case than for the k parameter. The maximal absolute values for the curves are 0.3115, 0.2474, and 0.2642 for the rainfall metrics of 1.0, 0.5, and -0.5 respectively. Furthermore the negative rainfall metric's maximal absolute value is now larger than the positive 0.5 rainfall metric, suggesting that the negative rainfall metric values will now be slightly greater than the positive. The order of most to least significant parameter for Eq.(4.16) when a positive rainfall metric is utilized is as follows: k, u, g, L, e, and a while for a negative rainfall metric the order becomes: g, u, e, L, k, and a. Thus the a parameter is once again the least significant parameter. The sensitivity of Eq.(4.16) appears to be more dependent on the sign of the rainfall metric as the ranking of the significance of each parameter is only constant for the u, L, and a parameters.

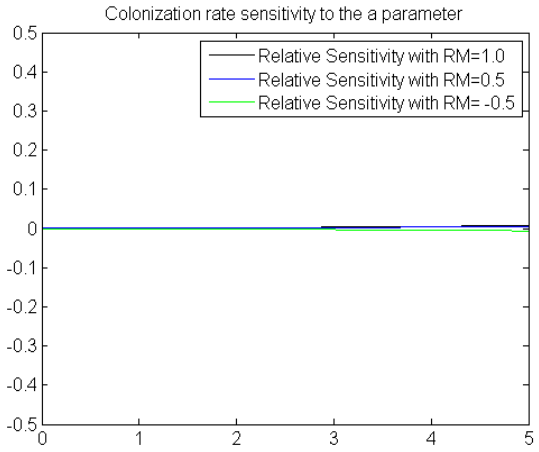

Figure 4.45: Colonization rate relative sensitivity to the a parameter with constant rainfall metrics.

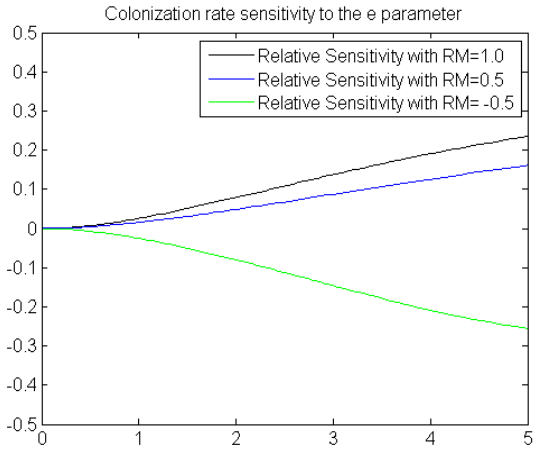

Figure 4.46: Colonization rate relative sensitivity to the e parameter with constant rainfall metrics.

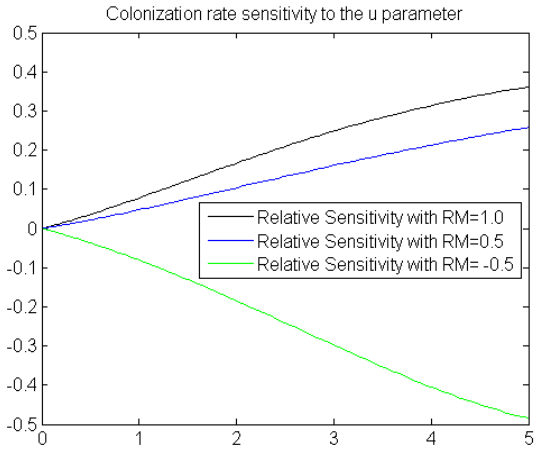

Figure 4.47: Colonization rate relative sensitivity to the u parameter with constant rainfall metrics.

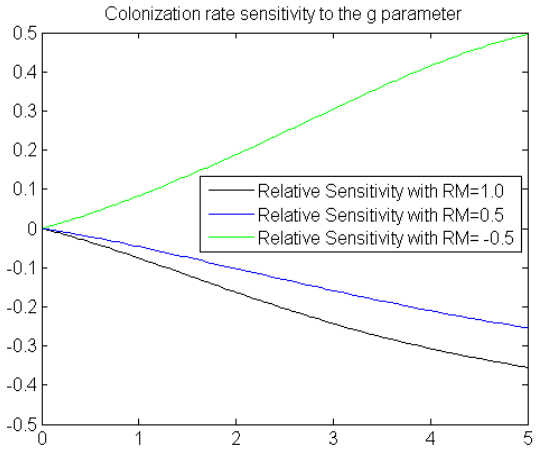

Figure 4.48: Colonization rate relative sensitivity to the g parameter with constant rainfall metrics.

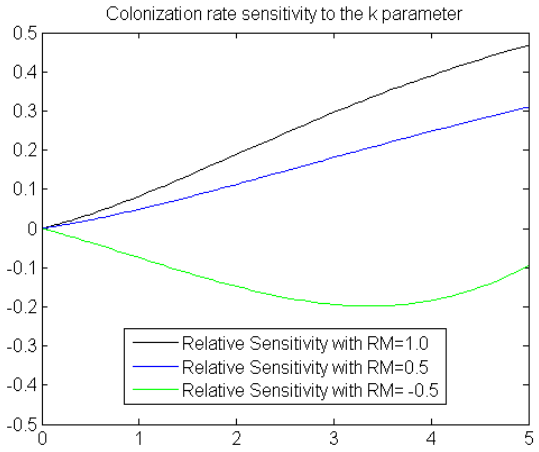

Figure 4.49: Colonization rate relative sensitivity to the k parameter with constant rainfall metrics.

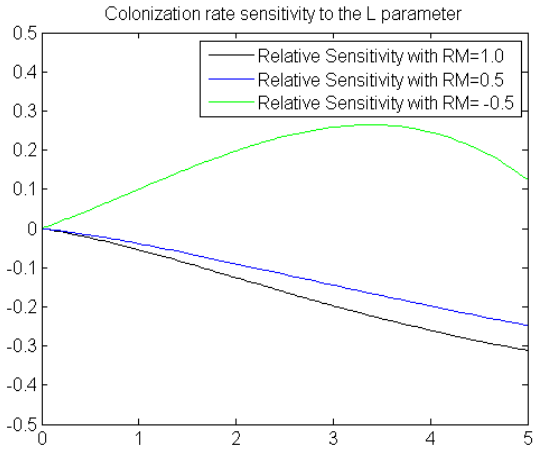

Figure 4.50: Colonization rate relative sensitivity to the L parameter with constant rainfall metrics.

Chapter 5

Discussion

To review, the model presented in this project was an attempt at incorporating the variability of both fecundity and colonization rate in order to describe the fraction of patches occupied of the northern spotted owl. The rainfall-fecundity relationship of the northern spotted owl motivated the development of a rainfall metric which was utilized to allow fecundity to depend on rainfall data. The colonization rate was transformed from a parameter in the Levins model to a variable in the new model which depended on the fraction of patches occupied, the fecundity, and the change in fecundity. Sensitivity analysis of the model was performed in order to rank the significance of the parameters found in the new model. The new model also had its parameters and initial conditions varied to show their effects as well as to demonstrate how important it is for good data to be available for these values.

In the Results chapter, it was demonstrated how this model does not adequately describe the cases where the fecundity has consistently negative behavior (resulting from the rainfall metric having consistently negative behavior) since larger values in fecundity will result in larger negative changes in both colonization rate and fraction of patches occupied. This behavior is contrary to the intuition that larger fecundity should result in larger values of colonization rate and fraction of patches occupied. Therefore it may be necessary for future work to develop the model further in order to accurately describe all cases, or even a complementary model to work when fecundity is consistently decreasing.

For the current model, it is important to find the origin of the parameters so that they may be measured in studies. From the sensitivity analysis performed it appears as though the most important parameters are g and u which are both consistently in the top three of significant parameters for both the negative and positive rainfall metrics. It would also be imperative to further study the initial conditions for the model. During the research for the construction of this model, there appeared to be a lack of data on colonization and extinction rates for the spotted owl. Since these values are integral to the Levins models it would be advisable to further investigate these values. The role of the colonization rates in the new model makes finding its true value even more important. The current dispersal rate data available might be utilized in order to identify appropriate colonization rates.

For future work it would also be important to attempt to incorporate even more of the available data for the spotted owls. This includes the extensive survivorship data which is accessible and categorized by age group. Since the younger owls have significantly lower survivorship, it might behoove future models to incorporate it.

Another component that should contribute to the value of the colonization and extinction parameters is dispersal rate. LaHaye et al. (1994) used a maximum dispersal rate of 4%, however, this value was determined to be too low for the model they chose as all populations tended towards extinction. Thomas (1990) measured dispersal rates for spotted owls and compared them to the distance between each patch in the study. This data can be seen in Fig. 5.1 and Fig. 5.2 respectively. The cumulative

distribution function in Fig. 5.3 shows what percentage of owls traveled each distance which, combined with a function describing the density of patches, may be used to develop into another parameter effecting both colonization and extinction rates. In addition to the cumulative distribution function which is based on field data, Fig. 5.4 shows the estimated dispersal rates (defined as the percentage of individuals migrating in each direction per year) used by LaHaye et al. (1994) in their model.

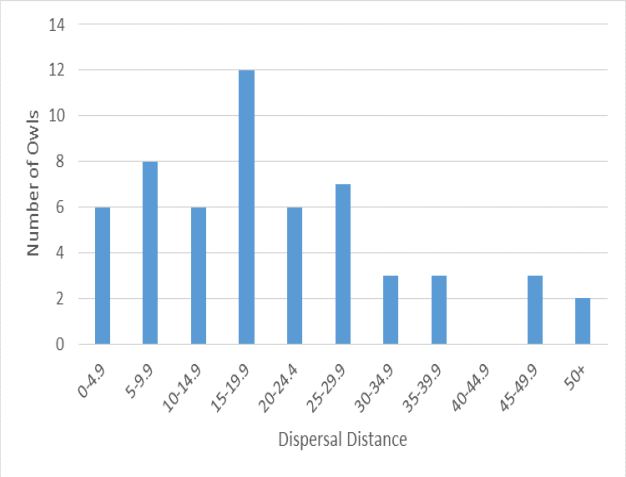

Figure 5.1: Frequency of dispersal distance of spotted owls from [34].

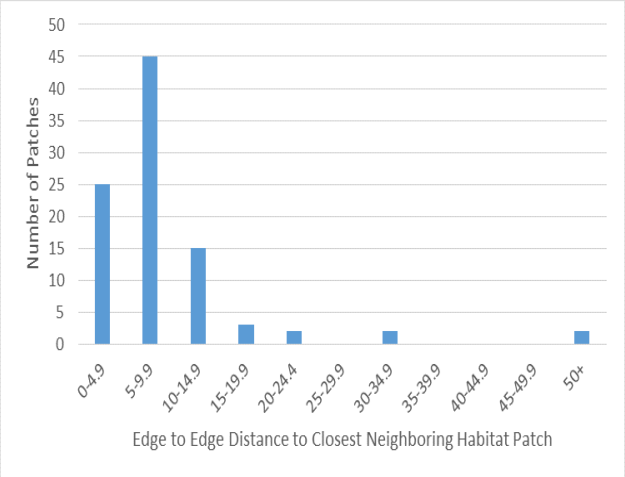

Figure 5.2: Frequency of habitat patches with varying edge to edge distances from [34].

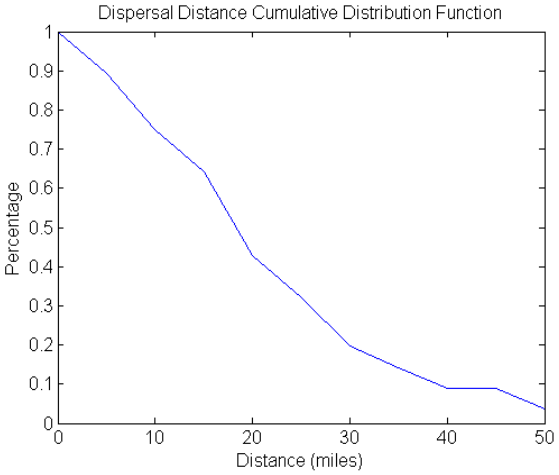

Figure 5.3: Cumulative distribution of dispersal distances of spotted owls from [34].

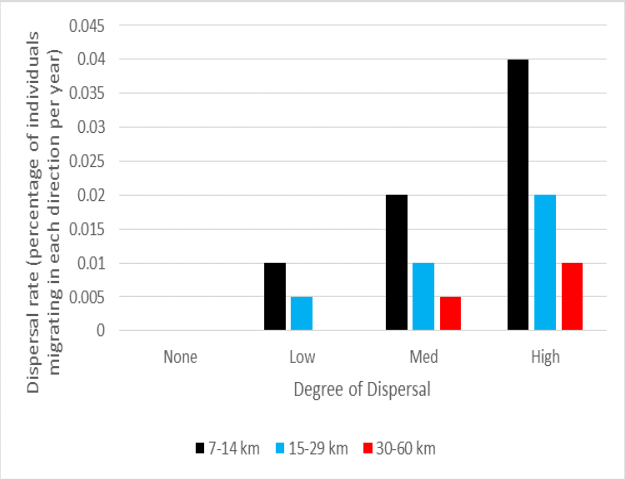

Figure 5.4: Estimated dispersal rates from [24].

The percentage of subadults in local populations by gender, as seen in Fig. 5.5, is one example of the data which could not easily be translated into components of either the colonization or fecundity terms developed. Additionally, Forsman (2011) revealed a breakdown of the composition of females by age which is important because the age at first breeding is usually two years old. This information, found in Fig. 5.6, could be useful for colonization rate when coupled with the fact that juveniles have a higher likelihood to disperse to new habitats where they would nest. The connection between age and fecundity is also explored in Fig. 5.7 which might be incorporated in future models similar in structure to the Lande model from Eq.(1.7). Blakesley et al. (2001) also found the nesting success for

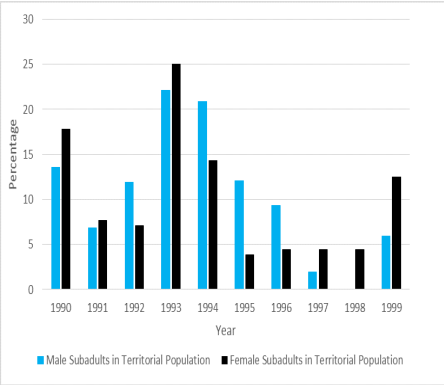

Figure 5.5: Percentage of male and female territorial California spotted owls in the subadult age classes in northeastern California, 1990-1999 (Graph and description from [6]).

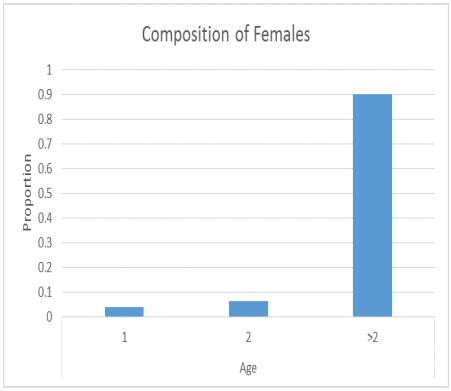

Figure 5.6: Composition of females by age in population from [10].

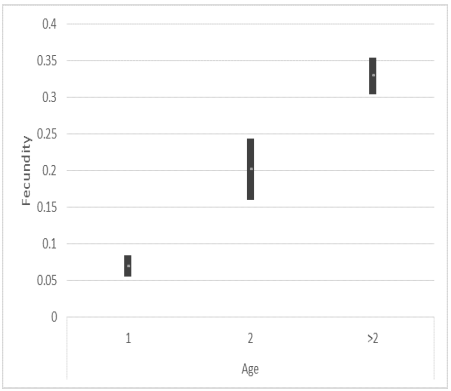

Figure 5.7: Fecundity ranges by age in population from [10].

spotted owls by year which may have an effect on fecundity. This data could be combined with the information from Fig. 5.8 which shows the difference in the percentage of females who fledged young (females who raised chicks to a fully grown state) by contrasting the percentage for all females against nesting females. In addition, there is also data available which describes the mean reproductive output for owls from southern California, New Mexico, and Arizona in Fig. 5.9 that may be used alongside or as an alternative to fecundity. Another direction could have been to observe the between-species interactions for the spotted owl with its prey and the competitor species the barred owl in order to determine the effects of non-anthropogenic causes on decline. Peery et al. (2012) focused on trends in climate change which when coupled with relationships like fecundity-rainfall could yield interesting conservation strategies in order to combat future problems. This study also included summaries of the mean minimum and mean maximum temperatures as well as mean precipitation (seen in Fig. 5.11, Fig. 5.12, and Fig. 5.13 respectively) from 1987 to 2001 for southern California, New Mexico, and Arizona. There is also data which can help to describe the local habitats. One such description comes in the form of a breakdown of spotted owl distribution by county (Fig. 5.16) as well as the ownership of the land where local habitats occur [16]. Furthermore there is data (Fig. 5.10) that describes the territory occupancy of patches in the San Bernadino Mountains which may be used to develop a model (or to judge a model's effectiveness) as one of the few examples of patch occupancy data available. This sort of data could shed light on where the best methods of conservation are originating in order to spread these techniques to the other areas. Parameters utilized by other models which can act as comparisons to identify appropriate ranges for future models can be seen in Fig. 5.14 and Fig. 5.15.

Figure 5.8: Proportion of only nesting females who fledged young as well as the proportion of all females who fledged young (data from [6]).

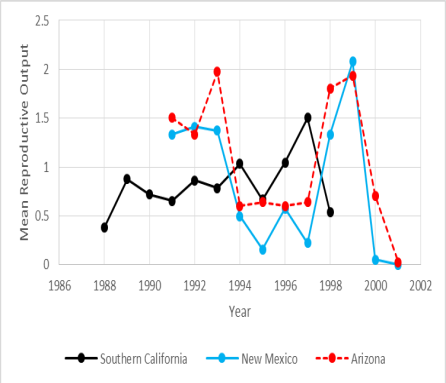

Figure 5.9: Estimated mean reproductive output from 1987 to 2001 taken from [29].

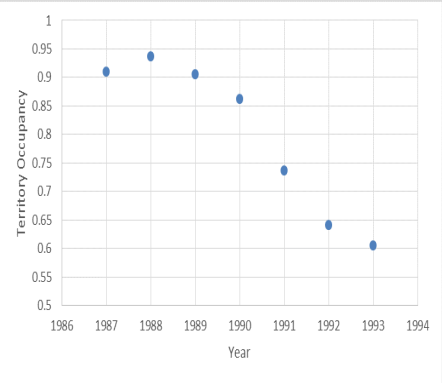

Figure 5.10: Territory occupancy in San Bernadino Mountains population found by [24].

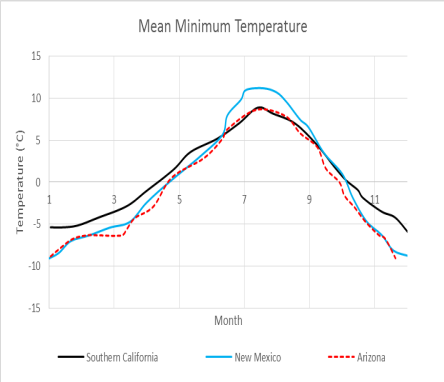

Figure 5.11: The mean minimum monthly temperatures (where 1 denotes January, 2 denotes February, etc.) from 1987 to 2001 taken from [29].

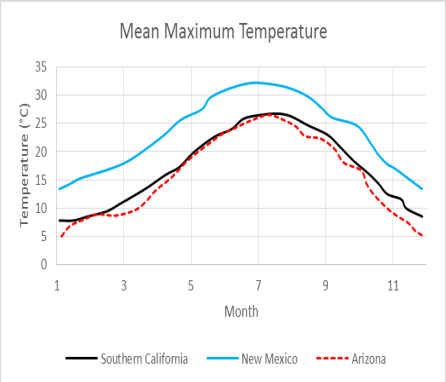

Figure 5.12: The mean maximum monthly temperatures (where 1 denotes January, 2 denotes February, etc.) from 1987 to 2001 taken from [29].

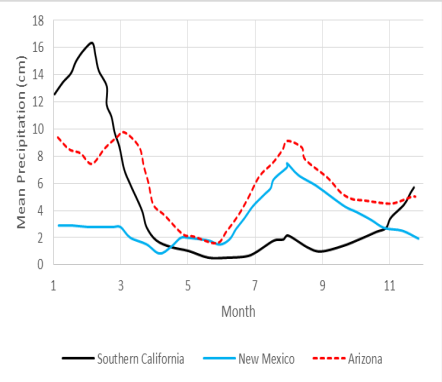

Figure 5.13: The mean monthly precipitation (where 1 denotes January, 2 denotes February, etc.) from 1987 to 2001 taken from [29].

Parameter Estimates		
Fledgling Survival Probability	0.6	
Juevenile Probability of Successful Dispersal	0.18	
Subadult Annual Survival Probability	0.77	
Adult Annual Survival Probability	0.92	0.9
Adult Female Average Annual Fecundity	0.33	
Age at First Breeding	2	
Current Percentage of Landscape Suitable	0.325	

Figure 5.14: Estimated values for parameters used in the model from [34].

Parameter[a]	Barrowclough and Coats (1985)	Draft EIS (USFS 1986)		Final EIS (USFS 1988)		Marcot and Holthausen (1987)	Lande (1988)	Noon and Biles (1990)
s_0	0.19	0.20	0.60	0.11	0.34	0.11	0.11	0.11
s_1	0.85	0.85	0.85	0.96	0.97	0.96	0.71	0.71
s		0.85	0.85	0.96	0.97	0.96	0.942	0.942
b	0.34	0.275	0.40	0.24	0.24	0.24	0.24	0.24
T	3	2	2	2	2	2	3	2 (3)
w	10	10	10	15	15	15	∞	∞ (16, 21, 26)
Estimates								
r	-0.237	-0.249	0.008	-0.164	-0.011	-0.170	-0.040	-0.040
λ	0.789	0.779	1.008	0.850	0.989	0.840	0.961	0.961

[a] b_0 = probability of survival to age 1 (first year survival rate); s_1 = probability of survival to age 2 (second year survival rate); s = annual survival rate from age 2 onward (ad survival rate); b = number of female fledglings produced by an adult female; T = age (yr) at first reproduction; w = age (yr) at reproductive senescence; r = intrinsic rate of natural increase (= ln λ).

Figure 5.15: From [28], this chart shows parameters used by various other models.

County	Present Number Known	Area (km^2)
Alpine	3	1924
Amador	6	1567
Butte	19	4343
Calaveras	11	2686
Colusa	2	2994
Del Norte	41	3186
El Dorado	75	4631
Fresno	23	15584
Glenn	12	3440
Humboldt	117	10495
Kern	13	21137
Lake	18	1327
Lassen	11	12225
Los Angeles	13	12308
Madera	24	5576
Marin	18	2145
Mariposa	29	3789
Mendocino	38	10044
Modoc	1	10886
Mono	1	3132
Monterey	9	9767
Napa	4	2041
Nevada	12	2523
Orange	2	2455
Placer	40	3893
Plumas	83	6768
Riverside	4	18910
San Bernardino	28	52072
San Diego	21	11722
San Luis Obispo	8	9365
Santa Barbara	17	9813
Shasta	36	9964
Sierra	27	10971
Siskiyou	250	16439
Sonoma	5	4579
Tehama	58	7672
Trinity	146	8309
Tulare	35	12595
Tuolumne	43	5890
Ventura	6	5720
Yuba	8	1668

Figure 5.16: Number of owls was taken from [16] while the size of the counties was found independently.

Bibliography

[1] *Historic Rainfall Data*, 2014 (accessed 3-13-15). `http://ocwatersheds.com/rainrecords/rainfalldata/historic_data/rainfall_data`.

[2] *Ordinary Differential Equations*, 2015 (accessed 3-13-15). `http://www.mathworks.com/help/matlab/math/ordinary-differential-equations.html`.

[3] Jonathan Bart. Amount of suitable habitat and viability of northern spotted owls. *Conservation Biology*, pages 943–946, 1995.

[4] Jonathan Bart and Eric D Forsman. Dependence of northern spotted owls strix occidentalis caurina on old-growth forests in the western usa. *Biological Conservation*, 62(2):95–100, 1992.

[5] Charles Bergman. *Should the government shoot the spotted owl's new enemy, the barred owl?*, 2013 (accessed 3-13-15). `http://www.slate.com/articles/health_and_science/animal_forecast/2013/02/spotted_owl_vs_barred_owl_will_the_forest_service_shoot_one_species_to_save.html`.

[6] Jennifer A Blakesley, Barry R Noon, and Daniel WH Shaw. Demography of the california spotted owl in northeastern california. *The Condor*, 103(4):667–677, 2001.

[7] Gerardo Ceballos, Andrés García, and Paul R Ehrlich. The sixth extinction crisis: loss of animal populations and species. *Journal of Cosmology*, 8(June):1821–1831, 2010.

[8] Jemery R Day and Hugh P Possingham. A stochastic metapopulation model with variability in patch size and position. *Theoretical Population Biology*, 48(3):333–360, 1995.

[9] Jared M Diamond. The island dilemma: lessons of modern biogeographic studies for the design of natural reserves. *Biological conservation*, 7(2):129–146, 1975.

[10] Eric Forsman. *Population Demography of Northern Spotted Owls: Published for the Cooper Ornithological Society*, volume 40. Univ of California Press, 2011.

[11] Michael Gilpin. Metapopulations and wildlife conservation: Approaches to modeling spatial structure. In Dale McCullough, editor, *Metapopulations and Wildlife Conservation*. Island Press, 1996.

[12] Nicholas J Gotelli. Metapopulation models: the rescue effect, the propagule rain, and the core-satellite hypothesis. *American Naturalist*, pages 768–776, 1991.

[13] Nicholas J Gotelli and Walter G Kelley. A general model of metapopulation dynamics. *Oikos*, pages 36–44, 1993.

[14] Sylvain Goutelle, Michel Maurin, Florent Rougier, Xavier Barbaut, Laurent Bourguignon, Michel Ducher, and Pascal Maire. The hill equation: a review of its capabilities in pharmacological modelling. *Fundamental & clinical pharmacology*, 22(6):633–648, 2008.

[15] R. Gutiérrez and Susan Harrison. Applying metapopulation theory to spotted owl management: A history and critique. In Dale McCullough, editor, *Metapopulations and Wildlife Conservation*. Island Press, 1996.

[16] Ralph J Gutierrez, Andrew B Carey, et al. Ecology and management of the spotted owl in the pacific northwest. 1985.

[17] DM Hamby. A review of techniques for parameter sensitivity analysis of environmental models. *Environmental monitoring and assessment*, 32(2):135–154, 1994.

[18] Ilkka Hanski. Single-species metapopulation dynamics: concepts, models and observations. *Biological Journal of the Linnean Society*, 42(1-2):17–38, 1991.

[19] Ilkka Hanski. A practical model of metapopulation dynamics. *Journal of animal ecology*, pages 151–162, 1994.

[20] Ilkka Hanski and Michael Gilpin. Metapopulation dynamics: brief history and conceptual domain. *Biological journal of the Linnean Society*, 42(1-2):3–16, 1991.

[21] Ilkka Hanski and Mats Gyllenberg. Two general metapopulation models and the core-satellite species hypothesis. *American Naturalist*, pages 17–41, 1993.

[22] Ilkka Hanski and Otso Ovaskainen. The metapopulation capacity of a fragmented landscape. *Nature*, 404(6779):755–758, 2000.

[23] Susan Harrison. Local extinction in a metapopulation context: an empirical evaluation. *Biological journal of the Linnean Society*, 42(1-2):73–88, 1991.

[24] William S LaHaye, RJ Gutiérrez, and H Resit Akcakaya. Spotted owl metapopulation dynamics in southern california. *Journal of Animal Ecology*, pages 775–785, 1994.

[25] Derek E Lee, Monica L Bond, and Rodney B Siegel. Dynamics of breeding-season site occupancy of the california spotted owl in burned forests. *The Condor*, 114(4):792–802, 2012.

[26] Dale McCullough. Introduction. In Dale McCullough, editor, *Metapopulations and Wildlife Conservation*. Island Press, 1996.

[27] Barry Noon and Kevin McKelvey. A common framework for conservation planning: Linking individual and metapopulation models. In Dale McCullough, editor, *Metapopulations and Wildlife Conservation*. Island Press, 1996.

[28] Barry R Noon and Charles M Biles. Mathematical demography of spotted owls in the pacific northwest. *The Journal of Wildlife Management*, pages 18–27, 1990.

[29] Marcus Zachariah Peery, Ralph J Gutiérrez, Rebecca Kirby, Olivia E LeDee, and William LaHaye. Climate change and spotted owls: potentially contrasting responses in the southwestern united states. *Global Change Biology*, 18(3):865–880, 2012.

[30] A Townsend Peterson and C Richard Robins. Using ecological-niche modeling to predict barred owl invasions with implications for spotted owl conservation. *Conservation Biology*, 17(4):1161–1165, 2003.

[31] Mary Price and Michael Gilpin. Modelers, mammalogists and metapopulations: Designing stephens' kangaroo rat reserves. In Dale McCullough, editor, *Metapopulations and Wildlife Conservation*. Island Press, 1996.

[32] Per Sjogren-Gulve and Chris Ray. Using logistic regression to model metapopulation dynamics: Large-scale forestry extirpates the pool frog. In Dale McCullough, editor, *Metapopulations and Wildlife Conservation*. Island Press, 1996.

[33] Bradley Smith, John Fitzpatrick, Glen Woolfenden, and Bill Pranty. Classification and conservation of metapopulations: A case study of the florida scrub jay. In Dale McCullough, editor, *Metapopulations and Wildlife Conservation*. Island Press, 1996.

[34] Jack Ward Thomas. *A conservation strategy for the northern spotted owl*. The Committee, 1990.

[35] Samuel K Wasser, Kenneth Bevis, Gina King, and Eric Hanson. Noninvasive physiological measures of disturbance in the northern spotted owl. *Conservation Biology*, 11(4):1019–1022, 1997.

[36] John Wiens. Wildlife in patchy environments: Metapopulations, mosaics, and management. In Dale McCullough, editor, *Metapopulations and Wildlife Conservation*. Island Press, 1996.